

MANIFOLD LEARNING IN METRIC SPACES

LIANE XU, AMIT SINGER

ABSTRACT. Laplacian-based methods are popular for dimensionality reduction of data lying in \mathbb{R}^N . Several theoretical results for these algorithms depend on the fact that the Euclidean distance approximates the geodesic distance on the underlying submanifold which the data are assumed to lie on. However, for some applications, other metrics, such as the Wasserstein distance, may provide a more appropriate notion of distance than the Euclidean distance. We provide a framework that generalizes the problem of manifold learning to metric spaces and study when a metric satisfies sufficient conditions for the pointwise convergence of the graph Laplacian.

1. INTRODUCTION

In the manifold learning problem in \mathbb{R}^N , we assume that data points $x_1, \dots, x_n \in \mathbb{R}^N$ are drawn i.i.d. from some probability distribution on an unknown compact, oriented submanifold $\mathcal{M} \subset \mathbb{R}^N$, and we would like to recover (properties of) \mathcal{M} . We can formulate an analogous problem of manifold learning in a metric space (X, d) as follows: let \mathcal{M} be a smooth, compact, oriented manifold, and let $\iota: \mathcal{M} \rightarrow X$ be an embedding. Given x_1, \dots, x_n drawn i.i.d. from some probability distribution on \mathcal{M} , what can we recover about \mathcal{M} ?

Several popular manifold learning algorithms for data points in \mathbb{R}^N — for example, Isomap [50], Laplacian eigenmaps [4, 5] and diffusion maps [19] — start by constructing a graph which depends on the pairwise Euclidean distances between the data points. To motivate why manifold learning in another metric space may be beneficial, consider the following example. Fix some $r > 0$. Let $\iota: \mathbb{S}^1 \rightarrow L^2(\mathbb{R}^2)$ be given by

$$\iota(\theta) := \frac{1}{\pi r^2} \mathbf{1}_{B_r((\cos \theta, \sin \theta))} \quad (1)$$

for $\theta \in [0, 2\pi)$, where $B_r(x)$ denotes an open ball of radius r centered at x and $\mathbf{1}_A$ denotes the indicator function for a set A . We can think of $\iota(\theta)$ (after some discretization) as an image of a ball of radius r centered at $(\cos \theta, \sin \theta)$. For a fine enough discretization, the Euclidean norm approximates the $L^2(\mathbb{R}^2)$ norm, up to a scaling factor.

We can explicitly compute the pairwise $L^2(\mathbb{R}^2)$ distances for this example. In fact, for $\theta, \varphi \in [0, 2\pi)$ and $r \in (0, 1]$, the angle between θ and φ is strictly greater than $2 \arcsin r$ if and only if $|(\cos \theta, \sin \theta) - (\cos \varphi, \sin \varphi)| > 2r$, and in this case,

$$\|\iota(\theta) - \iota(\varphi)\|_{L^2(\mathbb{R}^2)} = \frac{2}{r\sqrt{\pi}}$$

since the supports of $\iota(\theta)$ and $\iota(\varphi)$ are disjoint. Now suppose $\theta_1, \dots, \theta_n$ are drawn i.i.d. from the uniform distribution on $[0, 2\pi)$. If $|(\cos \theta_j, \sin \theta_j) - (\cos \theta_1, \sin \theta_1)| > 2r$ for all $j > 1$, then

$$\|\iota(\theta_j) - \iota(\theta_1)\|_{L^2(\mathbb{R}^2)} = \|\iota(\theta_i) - \iota(\theta_1)\|_{L^2(\mathbb{R}^2)}$$

Key words and phrases. Manifold learning, graph Laplacian, Laplacian eigenmaps, diffusion maps, Wasserstein space.

for all $i, j > 1$, so we have *no information* on the relative location of θ_1 compared to the other points. This happens with probability

$$\mathbb{P}(|(\cos \theta_j, \sin \theta_j) - (\cos \theta_1, \sin \theta_1)| > 2r \text{ for all } j > 1) = \left(1 - \frac{2 \arcsin r}{\pi}\right)^{n-1}.$$

Although this decays exponentially as $n \rightarrow \infty$, in practice, we may only have limited samples, so using the $L^2(\mathbb{R}^2)$ norm in this case would detrimentally affect the output of our algorithm (for Isomap, Laplacian eigenmaps, diffusion maps — *any* manifold learning algorithm that uses pairwise distances between data points), especially for small sample sizes and small r .

The issue here is that for small $r > 0$, the support of $\iota(\theta)$ is small for each $\theta \in [0, 2\pi)$. To alleviate this, we could consider using a different metric. For example, the Wasserstein-2 distance can also be computed explicitly: for $\theta, \varphi \in [0, 2\pi)$,

$$W_2^2(\iota(\theta), \iota(\varphi)) = |(\cos \theta, \sin \theta) - (\cos \varphi, \sin \varphi)|^2,$$

where, by a slight abuse of notation, we use $\iota(\theta)$ to denote the probability measure on \mathbb{R}^2 with density $\iota(\theta)$. For this example, the Wasserstein-2 distance provides a better notion of distance than the $L^2(\mathbb{R}^2)$ norm.

In this case, the use of the Wasserstein-2 metric with the embedding ι turns out to be equivalent to considering the typical embedding $\theta \mapsto (\cos \theta, \sin \theta)$ of \mathbb{S}^1 in \mathbb{R}^2 . However, more generally, we still lack a theoretical understanding of the use of non-Euclidean metrics in graph Laplacian-based manifold learning algorithms. Much work has been done in the Euclidean case (e.g., [4, 5, 6, 7, 8, 11, 16, 17, 19, 20, 29, 32, 48] and references therein), but less is known for other metrics [28, 30]. Kileel et al. [30] study the pointwise convergence of graph Laplacians with an arbitrary norm on \mathbb{R}^N , whereas Hamm et al. [28] study the Gromov-Wasserstein convergence of graph Laplacians with the Wasserstein-2 distance. To the best of our knowledge, the convergence of graph Laplacians with an arbitrary metric has not been studied before. Moreover, a theoretical understanding of why certain metrics produce better results for a given problem is also missing.

In this paper, we provide a partial answer. Henceforth, for convenience, we treat d as a metric on \mathcal{M} and write $d(x, y)$ instead of $d(\iota(x), \iota(y))$. Our first main contribution is proving that if \mathcal{M} is equipped with a Riemannian metric g , d_g is the associated geodesic distance and \exp is the exponential map, the following two assumptions suffice for the pointwise convergence of graph Laplacians:

Assumption 1 (Uniform first order approximation). The metric d satisfies the following relation with respect to the Riemannian metric g : as $t \rightarrow 0$,

$$\sup |d(x, \exp_x(tv)) - t| = o(t), \tag{2}$$

where the supremum is taken over all $(x, v) \in T\mathcal{M}$ satisfying $g_x(v, v) = 1$ and $|t| < \text{inj}_{(\mathcal{M}, g)}(x)$, where $\text{inj}_{(\mathcal{M}, g)}(x)$ is the injectivity radius at x .

Assumption 2. There exists $K, \varepsilon_0 > 0$ such that $d_g^2(x, y) - d^2(x, y) < Kd_g^4(x, y)$ for all $x, y \in \mathcal{M}$ such that $d_g(x, y) < \varepsilon_0$.

The benefits of this approach are twofold. First, Assumption 2 gives us a way to quantify how well d approximates d_g . Secondly, in contrast to [28, 30], these assumptions allow us to follow the proof of the pointwise convergence of graph Laplacians in the Euclidean case [6, 8] almost word-for-word; even more, this proof gives us upper bounds on the bias error in terms of K and ε_0 . This provides us with a better theoretical understanding of an observation that Kileel et al. made

with their numerical experiments [30, Section 5], which can be summarized roughly as follows: for two metrics d, \tilde{d} on a Riemannian manifold (\mathcal{M}, g) , if $y \mapsto d(x, y)$ and $y \mapsto \tilde{d}(x, y)$ both locally approximate $y \mapsto d_g(x, y)$, but $y \mapsto d(x, y)$ does so on a larger ball around x for all $x \in \mathcal{M}$, then the Laplacian eigenmaps algorithm tends to perform better with d than \tilde{d} .

Our second main contribution is observing that if d^2 is sufficiently regular around the diagonal of $\mathcal{M} \times \mathcal{M}$, then

$$g_x = \frac{1}{2} \text{Hess}_x (d^2(\cdot, x)) \quad \forall x \in \mathcal{M}$$

is the unique Riemannian metric on \mathcal{M} for which Assumptions 1 and 2 are satisfied. Here Hess_x denotes the Hessian evaluated at x , and $d^2(\cdot, x)$ denotes the map $y \mapsto d^2(y, x)$. (Since $d^2(\cdot, x)$ has a critical point at x , the Hessian can be taken with respect to any Riemannian metric on \mathcal{M} .) This allows us to more easily check when the graph Laplacians converge pointwise and to identify the limiting operator.

The rest of the paper is organized as follows. In Section 2, we provide some background on manifold learning and optimal transport and describe related work. In Section 3, we give conditions on d which are sufficient for the pointwise convergence of graph Laplacians. In Section 4, we provide several examples of when the Wasserstein-2 and other distances satisfy these conditions, and in Section 5, we perform numerical experiments which support our results from Section 3.

2. BACKGROUND

2.1. Manifold learning. We first briefly describe results from manifold learning in the Euclidean setting, with a focus on methods based on the graph Laplacian [4, 5, 6, 8, 19, 20, 32]. Let $\mathcal{M} \subset \mathbb{R}^N$ be a m -dimensional smooth, compact, oriented Riemannian submanifold of \mathbb{R}^N , and suppose we have data points x_1, \dots, x_n drawn i.i.d. uniformly from \mathcal{M} . In various applications, N may be large, and our goal is to perform dimensionality reduction, i.e., map each x_i into \mathbb{R}^l for $l \ll N$.

One popular method to do this is Laplacian eigenmaps, introduced by Belkin and Niyogi [4, 5]. For each $\varepsilon > 0$, define $k_\varepsilon: \mathbb{R}^N \times \mathbb{R}^N \rightarrow \mathbb{R}$ by

$$k_\varepsilon(x, y) := e^{-\frac{d(x, y)^2}{2\varepsilon}}, \tag{3}$$

where $d(x, y) = \|x - y\|_{\mathbb{R}^N}$, the typical Euclidean distance. Now construct a graph whose vertices are $\{x_i\}_{i \in [n]}$, and set the edge weight matrix $W \in \mathbb{R}^{n \times n}$ and degree matrix $D \in \mathbb{R}^{n \times n}$ via

$$W_{ij} = k_\varepsilon(x_i, x_j)$$

$$D_{ij} = \begin{cases} \sum_j W_{ij} & i = j \\ 0 & i \neq j \end{cases}$$

for $i, j \in [n]$.¹ The graph Laplacian $L^{(\varepsilon, n)}$ is then defined by

$$L^{(\varepsilon, n)} := D - W \tag{4}$$

and the (random walk) normalized graph Laplacian $\mathcal{L}^{(\varepsilon, n)}$ is given by

$$\mathcal{L}^{(\varepsilon, n)} := I - D^{-1}W. \tag{5}$$

¹In [4, 5], a δ -neighborhood rule or k NN rule is also used when constructing the adjacency graph, i.e., $W_{ij} = 0$ if $d(x_i, x_j)^2 \geq \delta$ (δ -neighborhood rule) or if x_j is not one of the k nearest neighbors of x_i (k NN rule). Following [6, 8], we do not do this; this simplifies our analysis, and we leave extensions to the δ -neighborhood or k NN case to future work.

More explicitly, for $f: \mathcal{M} \rightarrow \mathbb{R}$,

$$L^{(\varepsilon, n)} [f(x_i)]_i = \left[\sum_j k_\varepsilon(x_i, x_j) (f(x_i) - f(x_j)) \right]_i. \quad (6)$$

Hence we can define the discrete Laplacian $L^{(\varepsilon, n)} f$ of f by

$$L^{(\varepsilon, n)} f(x) := \sum_j k_\varepsilon(x, x_j) (f(x) - f(x_j)) \quad (7)$$

for $x \in \mathcal{M}$, and similarly,

$$\mathcal{L}^{(\varepsilon, n)} f(x) := \frac{\sum_j k_\varepsilon(x, x_j) f(x_j)}{\sum_j k_\varepsilon(x, x_j)} - f(x). \quad (8)$$

Since $D^{-1}W$ is a Markov transition matrix, it has an eigenvalue of 1 with eigenvector $[1 \cdots 1]^T$, and any other eigenvalue λ of $D^{-1}W$ satisfies $\lambda \leq 1$. It follows that $\mathcal{L}^{(\varepsilon, n)}$ has eigenvalues $\lambda_0, \dots, \lambda_{n-1}$ which satisfy

$$0 = \lambda_0 \leq \lambda_1 \leq \cdots \leq \lambda_{n-1},$$

with $v^{(0)} = [1 \cdots 1]^T$ the eigenvector for λ_0 . Laplacian eigenmaps then performs dimensionality reduction by computing the eigenvectors $v^{(1)}, \dots, v^{(l)}$ associated with $\lambda_1, \dots, \lambda_l$ and mapping each x_i into \mathbb{R}^l by

$$x_i \mapsto \begin{bmatrix} v_i^{(1)} \\ \vdots \\ v_i^{(l)} \end{bmatrix}. \quad (9)$$

The diffusion maps algorithm [19, 20, 32, 40] is similar in that it considers the spectral decomposition of the Markov transition matrix $D^{-1}W$ (or other normalizations of the weight matrix).

The theoretical motivation for these graph Laplacian-based methods lies in the fact that the graph Laplacian approximates (in several senses, to be made precise later) the Laplace-Beltrami operator on \mathcal{M} . Recall that for a Riemannian manifold (\mathcal{M}, g) and smooth vector fields X, Y on \mathcal{M} , the Hessian of $f \in C^\infty(\mathcal{M})$ is given by

$$\text{Hess}f(X, Y) := X(Yf) - df(\nabla_X Y), \quad (10)$$

where ∇ is the Levi-Civita connection on (\mathcal{M}, g) , and the Laplace-Beltrami operator Δ_g is the negative of the trace of the Hessian:

$$\Delta_g f := -\text{Tr}(\text{Hess}f). \quad (11)$$

Notably, on a compact, connected oriented Riemannian manifold (\mathcal{M}, g) , there exist smooth eigenfunctions $\{\varphi^{(k)}\}_{k \in \mathbb{Z}_{\geq 0}}$ of Δ_g such that $\{\varphi^{(k)}\}_{k \in \mathbb{Z}_{\geq 0}}$ is an orthonormal basis of $L^2(\mathcal{M})$, $\varphi^{(0)}$ is constant on \mathcal{M} and the associated eigenvalues $\{\lambda_k\}_{k \in \mathbb{Z}_{\geq 0}}$ are ordered:

$$0 = \lambda_0 < \lambda_1 \leq \cdots \leq \lambda_k \leq \lambda_{k+1} \leq \cdots.$$

See, e.g., [43] for a proof and further discussion of the importance of the Laplace-Beltrami operator on Riemannian manifolds. As an example, for $\mathcal{M} = \mathbb{S}^1$, we can take $\{\varphi^{(k)}\}_{k \in \mathbb{Z}_{\geq 0}}$ to be the Fourier basis, ordered by increasing frequency. As a corollary,

$$x \mapsto \left[\varphi^{(k)}(x) \right]_{k \in \mathbb{N}} \quad (12)$$

is an injective map on \mathcal{M} [10], and in fact, it suffices to take finitely many eigenfunctions: there exists $\bar{l} < \infty$ such that

$$x \mapsto \left[\varphi^{(k)}(x) \right]_{k \in [\bar{l}]} \tag{13}$$

is a smooth embedding of \mathcal{M} into $\mathbb{R}^{\bar{l}}$ [1, 3, 9]. (9) can then be viewed as a discrete approximation of (13).

More precisely, if (\mathcal{M}, g) is a smooth, compact, oriented m -dimensional Riemannian submanifold of \mathbb{R}^N , x_1, x_2, \dots, x_n are drawn i.i.d. from the uniform distribution on \mathcal{M} , $\varepsilon_n = 2n^{-\frac{1}{m+2+\alpha}}$ for some $\alpha > 0$, $x \in \mathcal{M}$ and $f \in C^\infty(\mathcal{M})$, then Belkin and Niyogi showed that

$$\frac{2}{\varepsilon_n (2\pi\varepsilon_n)^{m/2} n} L^{(\varepsilon_n, n)} f(x) \rightarrow \frac{\Delta_g f(x)}{\text{vol}(\mathcal{M})} \tag{14}$$

in probability as $n \rightarrow \infty$ [6, 8]. A similar result can be shown for normalized graph Laplacians; the convergence rate was studied in [29, 48]. Belkin and Niyogi also established spectral convergence when x_1, x_2, \dots, x_n are drawn from the uniform distribution on \mathcal{M} [7].

More generally, if x_1, x_2, \dots, x_n are drawn from a probability distribution on \mathcal{M} with density $P \in C^3(\mathcal{M})$, the limit in (14) is instead $P\Delta_g f - 2\langle \text{grad}_g f, \text{grad}_g P \rangle$ [8, 19, 20, 29, 32, 40]. Spectral convergence (with convergence rates) was studied in this setting in [17, 25]. We note that several of the aforementioned works (e.g., [17, 19, 20, 25, 29]) and many other works (e.g., [14, 15, 16, 51] and references therein) also establish convergence results for several variants of graph Laplacians; for example, for kernels other than the Gaussian kernel (3), for normalizations other than the random walk normalization (5), for graphs constructed with the δ -neighborhood rule or k NN rule, etc. For simplicity, we only consider the graph Laplacian and its random walk normalization as we have introduced them in (4) and (5) respectively, and leave extensions to other variants of the graph Laplacian to future work.

2.2. Optimal transport. As noted in the introduction, one of the metrics that we are interested in is the Wasserstein distance. Let $\mathcal{P}(X)$ denote the set of Borel probability measures on a metric space X , and for $p \geq 1$, let $\mathcal{P}_p(\mathbb{R}^N)$ denote the set of Borel probability measures with finite p th moments on \mathbb{R}^N . The Wasserstein- p distance $W_p(\mu, \nu)$ between $\mu, \nu \in \mathcal{P}_p(\mathbb{R}^N)$ is given by

$$W_p(\mu, \nu) := \inf_{\gamma \in \Gamma_{\mu, \nu}} \left(\int_{\mathbb{R}^N} \|x - y\|^p d\gamma(x, y) \right)^{1/p}, \tag{15}$$

where $\Gamma_{\mu, \nu}$ is the set of couplings between μ and ν , i.e., the set of probability measures $\gamma \in \mathcal{P}(\mathbb{R}^N \times \mathbb{R}^N)$ whose first marginal is μ and second marginal is ν .

We will mainly be concerned with the case $p = 2$ because $(\mathcal{P}_2(\mathbb{R}^N), W_2)$ has a formal Riemannian structure. If we can embed a manifold \mathcal{M} into $(\mathcal{P}_2(\mathbb{R}^N), W_2)$ and equip it with this formal Riemannian structure, then we can understand \mathcal{M} (at least formally) as a *Riemannian* submanifold of $(\mathcal{P}_2(\mathbb{R}^N), W_2)$. If this turns out to be an actual Riemannian metric g on \mathcal{M} , we can then ask when the graph Laplacians converge to the Laplace-Beltrami operator Δ_g induced by g , in direct analogy with the manifold learning problem in Euclidean space.

In what follows, we briefly review the formal Riemannian structure of $(\mathcal{P}_2(\mathbb{R}^N), W_2)$. For more details, we refer the reader to [2]. For more on optimal transport more broadly, we refer the reader to one of several books on optimal transport, e.g., [44, 52, 53].

2.2.1. Riemannian structure of Wasserstein space. Let (X, d) be a complete metric space and $I = (a, b)$ for some $a < b$. Recall that a curve $\gamma: I \rightarrow X$ is absolutely continuous if there exists $f \in L^1(I)$ such that

$$d(\gamma(s), \gamma(t)) \leq \int_s^t f(x) dx \quad (16)$$

for all $s, t \in I$ such that $s \leq t$ [2, Definition 1.1.1]. Moreover, if γ is absolutely continuous, the metric derivative, defined as

$$|\gamma'| (t) := \lim_{\varepsilon \rightarrow 0} \frac{d(\gamma(t + \varepsilon), \gamma(t))}{|\varepsilon|},$$

exists for a.e. $t \in I$ and $|\gamma'| \in L^1(I)$ [2, Theorem 1.1.2].

In the case when $(X, d) = (\mathcal{P}_2(\mathbb{R}^N), W_2)$, it can be shown [2, Theorem 8.3.1] that any absolutely continuous curve

$$\begin{aligned} \mu: I &\rightarrow \mathcal{P}_2(\mathbb{R}^N) \\ t &\mapsto \mu_t \end{aligned}$$

admits a Borel measurable time-dependent vector field

$$\begin{aligned} v: \mathbb{R}^N \times I &\rightarrow \mathbb{R}^N \\ (x, t) &\mapsto v_t(x) \end{aligned}$$

such that

- the continuity equation

$$\frac{\partial \mu}{\partial t} + \operatorname{div}(v_t \mu_t) = 0$$

is satisfied in the distributional sense:

$$\int_I \int_{\mathbb{R}^N} \frac{\partial \varphi}{\partial t} + \langle v_t, \nabla \varphi \rangle d\mu_t dt = 0 \quad (17)$$

- for every $\varphi \in C_c^\infty(\mathbb{R}^N \times I)$, where ∇ is the gradient on \mathbb{R}^N ;
- $v_t \in L^2(\mu_t)$ and $\|v_t\|_{L^2(\mu_t)} = |\mu'| (t)$ for a.e. $t \in I$;
- $v_t \in \overline{\{\nabla \varphi: \varphi \in C_c^\infty(\mathbb{R}^N)\}}^{L^2(\mu_t)}$ for a.e. $t \in I$, where $\overline{V}^{L^2(\mu_t)}$ denotes the closure of $V \subset L^2(\mu_t)$ in $L^2(\mu_t)$.

On the other hand, suppose a Borel measurable vector field $v: \mathbb{R}^N \times I \rightarrow \mathbb{R}^N$ satisfies the continuity equation in the distributional sense and $t \mapsto \|v_t\|_{L^2(\mu_t)}$ belongs to $L^1(I)$. Then

$$|\mu'| (t) \leq \|v_t\|_{L^2(\mu_t)}$$

for a.e. $t \in I$ [2, Theorem 8.3.1]. In other words, there exists a time-dependent vector field $\{v_t\}_{t \in I}$ satisfying the continuity equation whose $L^2(\mu_t)$ norm is minimal and agrees with the metric derivative for a.e. $t \in I$.

In addition, if both $v: \mathbb{R}^N \times I \rightarrow \mathbb{R}^N$ and $\tilde{v}: \mathbb{R}^N \times I \rightarrow \mathbb{R}^N$ are Borel measurable, satisfy the continuity equation and $v_t, \tilde{v}_t \in \overline{\{\nabla \varphi: \varphi \in C_c^\infty(\mathbb{R}^N)\}}^{L^2(\mu_t)}$ for a.e. $t \in I$, then $v_t = \tilde{v}_t$ for a.e. $t \in I$. Indeed, since v and \tilde{v} both satisfy the continuity equation, their difference is divergence-free:

$$\operatorname{div}((v_t - \tilde{v}_t)\mu_t) = 0$$

for a.e. $t \in I$. By definition, for any $\nu \in \mathcal{P}_2(\mathbb{R}^N)$ and vector field $w \in L^2(\nu)$, $\operatorname{div}(w\nu) = 0$ means that

$$\langle \nabla \varphi, w \rangle_{L^2(\nu)} = 0$$

for all $\varphi \in C_c^\infty(\mathbb{R}^N)$, so the orthogonal complement of $\{w: \operatorname{div}(w\nu) = 0\}$ in $L^2(\nu)$ is

$$\{w: \operatorname{div}(w\nu) = 0\}^\perp = \overline{\{\nabla\varphi: \varphi \in C_c^\infty(\mathbb{R}^N)\}}^{L^2(\nu)}.$$

Hence $v_t = \tilde{v}_t$ for a.e. $t \in I$. Altogether, this motivates the definition for the tangent space at $\nu \in \mathcal{P}_2(\mathbb{R}^N)$:

$$T_\nu \mathcal{P}_2(\mathbb{R}^N) := \overline{\{\nabla\varphi: \varphi \in C_c^\infty(\mathbb{R}^N)\}}^{L^2(\nu)}.$$

The formal Riemannian structure of $\mathcal{P}_2(\mathbb{R}^N)$ is then obtained by taking the $L^2(\nu)$ inner product on $T_\nu \mathcal{P}_2(\mathbb{R}^N)$ for each $\nu \in \mathcal{P}_2(\mathbb{R}^N)$.

2.3. Related work. The idea of using other metrics in graph Laplacian-based methods for dimensionality reduction is not new. Zelesko et al. proposed using a wavelet approximation of the Wasserstein-1 metric [47] in the diffusion maps algorithm [55] (see also [30]) to study the conformation space of a molecule. Lu et al. used the diffusion maps algorithm with the Wasserstein-2 metric to identify conserved quantities in a dynamical system [37]. Several works have also looked at extending other dimensionality reduction methods to a space of probability measures equipped with the Wasserstein distance (or approximations thereof) [12, 21, 24, 27, 46]. Additionally, Mishne et al. defined a metric based on a tree constructed from the data and used this metric in the diffusion maps algorithm to analyze neuronal activity [38]. However, for this paper, we assume that the metric is independent of the data, so our results do not apply to the metric used in [38].

The two works closest to ours are [30] and [28]. Kileel et al. [30] establish pointwise convergence of the graph Laplacian to a Laplacian-like operator when \mathcal{M} is a smooth submanifold of \mathbb{R}^N with an arbitrary norm. In contrast, we do not require \mathcal{M} to be a submanifold of \mathbb{R}^N , and we consider metrics, not just norms. Moreover, the coefficients of the limiting operator in [30] are given in terms of extrinsic quantities such as the second fundamental form, whereas the limiting operators in Theorem 3.1 and Theorem 3.2 are intrinsic. In some cases, we can show that their limiting operator is the same as ours; we provide an example of this in Section 4.1. However, the assumptions we make (Assumptions 1 and 2) may not be satisfied by an arbitrary norm and smooth submanifold of \mathbb{R}^N .

On the other hand, Hamm et al. [28] focus on the space of absolutely continuous probability measures $\mathcal{P}_{ac}(\Omega)$ on a compact, convex subset $\Omega \subset \mathbb{R}^N$ equipped with the Wasserstein-2 distance W_2 . They prove convergence of graph Laplacians in the Gromov-Wasserstein sense when there is a bi-Lipschitz embedding (with some additional regularity conditions) of a compact, connected smooth Riemannian manifold (\mathcal{M}, g) into $(\mathcal{P}_{ac}(\Omega), W_2)$. Although we require stricter conditions (for one, we require W_2 to be a first-order approximation of the geodesic distance on (\mathcal{M}, g) ; see Assumptions 1 and 2 for more precise statements), this allows us to prove pointwise convergence of graph Laplacians and also gives us the nice interpretation of \mathcal{M} as a (formal) *Riemannian* submanifold of Wasserstein-2 space. Moreover, two of their examples [28, Examples 2.4 and 2.5] fall under our assumptions as well. We discuss the Wasserstein-2 space in Section 4.2.

2.4. Notation and assumptions. All of our results in Section 3 hold when \mathcal{M} is a smooth, compact, oriented manifold. It is possible to assume looser conditions: for example, following more or less the same proof, Theorem 3.1 also holds when \mathcal{M} is just a subset of finite volume of a smooth, oriented Riemannian manifold $(\tilde{\mathcal{M}}, g)$ and x belongs to the interior of \mathcal{M} . However, for simplicity, we take \mathcal{M} to be a smooth, oriented manifold. We will provide an example of a non-compact manifold in Section 4.1, so we do not require compactness.

When we say that d is a metric on \mathcal{M} , we mean that there exists an *embedding* $\iota: \mathcal{M} \rightarrow (X, d)$ of \mathcal{M} into a metric space (X, d) . If \mathcal{M} is compact, then any injective continuous map $\iota: \mathcal{M} \rightarrow X$ is an embedding. However, if \mathcal{M} is not compact, this is not true. That ι is a homeomorphism between \mathcal{M} and $\iota(\mathcal{M})$, where $\iota(\mathcal{M})$ is equipped with the subspace topology, is required for our results in Section 3.1 to hold.

We warn the reader that we will make different assumptions for \mathcal{M} in Section 3.1 and Section 3.2:

- In Section 3.1, we equip \mathcal{M} with a Riemannian metric g and its Levi-Civita connection. We assume that \mathcal{M} has finite volume with respect to g and that g is C^{k+1} for some $k \in \mathbb{N}$, $k \geq 3$. We denote the geodesic distance on (\mathcal{M}, g) by d_g . The volume form is denoted by dV_g , and the volume of \mathcal{M} is denoted by $\text{vol}_g(\mathcal{M})$. The gradient is denoted by grad_g . As in (10) and (11), let Hess and Δ_g denote, respectively, the Hessian and Laplacian on (\mathcal{M}, g) . Since g is C^{k+1} , the exponential map \exp is C^k around $\mathcal{M} \times \{0\} \subset T\mathcal{M}$ (see, e.g., [33]). We denote the injectivity radius at $x \in \mathcal{M}$ by

$$\text{inj}_{(\mathcal{M}, g)}(x) := \sup\{\delta > 0: \exp_x \text{ is a } C^k\text{-diffeomorphism on } B_\delta(0)\}. \quad (18)$$

- In Section 3.2, a priori, we do not equip \mathcal{M} with a Riemannian metric. Rather, we show that if d is a metric on \mathcal{M} and d^2 is sufficiently regular around the diagonal of $\mathcal{M} \times \mathcal{M}$,

$$g_x = \frac{1}{2} \text{Hess}_x(d^2(\cdot, x))$$

is the unique Riemannian metric on \mathcal{M} such that the results of Section 3.1 hold. Here $d^2(\cdot, x)$ denotes the map $y \mapsto d^2(y, x)$. Since $d^2(\cdot, x)$ has a critical point at x , the Hessian can be taken with respect to any Riemannian metric on \mathcal{M} ; in other words, by (10), if x is a critical point of f ,

$$\text{Hess}_x f(X, Y) = X(Yf)(x)$$

for smooth vector fields X, Y on \mathcal{M} , independent of any Riemannian metric on \mathcal{M} . We denote the diagonal of $\mathcal{M} \times \mathcal{M}$ by

$$D_{\mathcal{M}} := \{(x, x): x \in \mathcal{M}\}.$$

Throughout the paper, unless otherwise stated, m is the dimension of \mathcal{M} , and n is the sample size.

3. POINTWISE CONVERGENCE OF THE GRAPH LAPLACIAN

Let us start from the Euclidean case. Consider a smooth oriented Riemannian submanifold (\mathcal{M}, g) of \mathbb{R}^N of finite volume. Let $x \in \mathcal{M}$ and $f \in C^3(\mathcal{M}) \cap L^\infty(\mathcal{M})$. Suppose x_1, \dots, x_n are drawn i.i.d. from the uniform distribution on (\mathcal{M}, g) . The proof of the pointwise convergence of graph Laplacians in (14) can be broken into two parts [6, 8].

One part follows from standard techniques in concentration of measure. Defining the random variables $X_j^{(\varepsilon)} := k_\varepsilon(x, x_j)$, $Y_j^{(\varepsilon)} := k_\varepsilon(x, x_j)f(x_j)$, we can express $L^{(\varepsilon, n)}f(x)$ as

$$L^{(\varepsilon, n)}f(x) = \sum_{j=1}^n f(x)X_j^{(\varepsilon)} - Y_j^{(\varepsilon)}.$$

Since $f(x)X_1^{(\varepsilon)} - Y_1^{(\varepsilon)}, \dots, f(x)X_n^{(\varepsilon)} - Y_n^{(\varepsilon)}$ are independent and $|f(x)X_j^{(\varepsilon)} - Y_j^{(\varepsilon)}| \leq 2\|f\|_\infty$ almost surely, by Hoeffding's inequality,

$$\mathbb{P}\left(\left|\frac{L^{(\varepsilon,n)}f(x)}{n} - \mathbb{E}\left[f(x)X_1^{(\varepsilon)} - Y_1^{(\varepsilon)}\right]\right| > \delta\right) \leq 2e^{-\frac{n\delta^2}{8\|f\|_\infty^2}}.$$

If $\varepsilon_n = 2n^{-\frac{1}{m+2+\alpha}}$ for some $\alpha > 0$,

$$\mathbb{P}\left(\frac{2}{\varepsilon_n(2\pi\varepsilon_n)^{m/2}}\left|\frac{L^{(\varepsilon_n,n)}f(x)}{n} - \mathbb{E}\left[f(x)X_1^{(\varepsilon_n)} - Y_1^{(\varepsilon_n)}\right]\right| > \delta\right) \leq 2e^{-\frac{n(\delta(2\pi\varepsilon_n)^{m/2}\varepsilon_n/2)^2}{8\|f\|_\infty^2}} \quad (19)$$

goes to 0 as $n \rightarrow \infty$. Moreover, for $\varepsilon_n = \Omega\left(n^{-\frac{1}{m+2+\alpha}}\right)$ and any $\delta > 0$,

$$\sum_{n \in \mathbb{N}} 2e^{-\frac{n(\delta(2\pi\varepsilon_n)^{m/2}\varepsilon_n/2)^2}{8\|f\|_\infty^2}} < \infty,$$

so by Borel-Cantelli, $\mathbb{P}(E_\delta) = 1$, where E_δ is the event

$$E_\delta := \left\{ \exists L \text{ such that } \frac{2}{\varepsilon_n(2\pi\varepsilon_n)^{m/2}} \left| \frac{L^{(\varepsilon_n,n)}f(x)}{n} - \mathbb{E}\left[f(x)X_1^{(\varepsilon_n)} - Y_1^{(\varepsilon_n)}\right] \right| \leq \delta \forall n \geq L \right\}.$$

Hence

$$\mathbb{P}\left(\frac{2}{\varepsilon_n(2\pi\varepsilon_n)^{m/2}} \left| \frac{L^{(\varepsilon_n,n)}f(x)}{n} - \mathbb{E}\left[f(x)X_1^{(\varepsilon_n)} - Y_1^{(\varepsilon_n)}\right] \right| \xrightarrow{n \rightarrow \infty} 0\right) = \mathbb{P}\left(\bigcap_{M \in \mathbb{N}} E_{1/M}\right) = 1.$$

Therefore, to prove that

$$\frac{2}{\varepsilon_n(2\pi\varepsilon_n)^{m/2}n} L^{(\varepsilon_n,n)}f(x) \rightarrow \frac{\Delta_g f(x)}{\text{vol}_g(\mathcal{M})} \quad (20)$$

almost surely as $n \rightarrow \infty$, it suffices to prove that

$$\lim_{n \rightarrow \infty} \frac{2\mathbb{E}\left[f(x)X_1^{(\varepsilon_n)} - Y_1^{(\varepsilon_n)}\right]}{\varepsilon_n(2\pi\varepsilon_n)^{m/2}} = \frac{\Delta_g f(x)}{\text{vol}_g(\mathcal{M})}. \quad (21)$$

Remark 3.1. *We have not used any properties of the uniform distribution or the Euclidean distance so far; (19) holds even if x_1, \dots, x_n are drawn i.i.d. from any probability distribution on \mathcal{M} and if we replace the Euclidean distance with any metric d on \mathcal{M} (see also [30, Section 4.1]).*

The second part of proving the pointwise convergence of graph Laplacians (14) is to prove (21). This relies on the following property of the Euclidean distance and geodesic distance d_g on \mathcal{M} [8, Lemma 4.3]: there exists a constant $K > 0$ such that

$$\|x - y\|^2 \leq d_g^2(x, y) \leq \|x - y\|^2 + Kd_g^4(x, y) \quad (22)$$

for all $x, y \in \mathcal{M}$. Therefore, more generally, if (\mathcal{M}, g) is a Riemannian manifold of finite volume, d is a metric on \mathcal{M} and there exists $K > 0$ such that

$$d^2(x, y) \leq d_g^2(x, y) \leq d^2(x, y) + Kd_g^4(x, y) \quad (23)$$

for all $x, y \in \mathcal{M}$, then Belkin and Niyogi's proof of the pointwise convergence of graph Laplacians (14), *mutatis mutandis*, still holds. A careful reading of the proof in [6, 8] shows that it suffices for (23) to hold locally, as we detail in the next section.

3.1. Sufficient conditions for convergence of the graph Laplacian. Suppose \mathcal{M} is a smooth oriented manifold equipped with a C^{k+1} Riemannian metric g for some $k \in \mathbb{N}$ such that $k \geq 3$, and suppose also that (\mathcal{M}, g) has finite volume. Recall the following assumptions mentioned in the introduction:

Assumption 1 (Uniform first order approximation). The metric d satisfies the following relation with respect to the Riemannian metric g : as $t \rightarrow 0$,

$$\sup |d(x, \exp_x(tv)) - t| = o(t), \quad (2)$$

where the supremum is taken over all $(x, v) \in T\mathcal{M}$ satisfying $g_x(v, v) = 1$ and $|t| < \text{inj}_{(\mathcal{M}, g)}(x)$, where $\text{inj}_{(\mathcal{M}, g)}(x)$ is the injectivity radius at x .

Assumption 2. There exists $K, \varepsilon_0 > 0$ such that $d_g^2(x, y) - d^2(x, y) < Kd_g^4(x, y)$ for all $x, y \in \mathcal{M}$ such that $d_g(x, y) < \varepsilon_0$.

To draw a parallel with (23), we prove that if Assumption 1 holds, then the lower bound in (23) holds locally.

Lemma 3.1. *Assumption 1 implies $d(x, y) \leq d_g(x, y)$ for all $x, y \in \mathcal{M}$ such that $d_g(x, y) < \text{inj}_{(\mathcal{M}, g)}(x)$.*

Proof. If (2) holds, then for any $t \in (0, \text{inj}_{\mathcal{M}}(x))$ and $(x, v) \in T\mathcal{M}$ such that $g_x(v, v) = 1$,

$$d(x, \exp_x(tv)) \leq \liminf_{N \rightarrow \infty} \sum_{i \in [N]} d\left(\exp_x\left(\frac{t(i-1)}{N}\right), \exp_x\left(\frac{ti}{N}\right)\right) \leq t = d_g(x, \exp_x(tv)).$$

This implies that

$$d(x, y) \leq d_g(x, y)$$

for all $x, y \in \mathcal{M}$ such that $d_g(x, y) < \text{inj}_{(\mathcal{M}, g)}(x)$. \square

Assumption 2 can be seen as a local version of the upper bound in (23). We claim that Assumptions 1 and 2 allow us to generalize Belkin and Niyogi's result [8, Theorem 3.1] on the pointwise convergence of graph Laplacians almost word-for-word.

Theorem 3.1. *Suppose that Assumptions 1 and 2 are satisfied, and that x_1, \dots, x_n are drawn i.i.d. uniformly from \mathcal{M} (with respect to g). Fix any $f \in C^3(\mathcal{M}) \cap L^\infty(\mathcal{M})$ and $x \in \mathcal{M}$. If $\varepsilon_n = 2n^{-\frac{1}{m+2+\alpha}}$ for some $\alpha > 0$, then*

$$\frac{2}{\varepsilon_n(2\pi\varepsilon_n)^{m/2}n} L^{(\varepsilon_n, n)} f(x) \rightarrow \frac{\Delta_g f(x)}{\text{vol}_g(\mathcal{M})}$$

almost surely as $n \rightarrow \infty$.

From our discussion at the beginning of the section, to prove Theorem 3.1, it suffices to prove (21) with the Euclidean distance replaced by a metric d satisfying Assumptions 1 and 2. For each $\varepsilon > 0$, define the operator G_ε by²

$$G_\varepsilon f(x) := \frac{\text{vol}(\mathcal{M}) \mathbb{E} \left[Y_1^{(\varepsilon)} \right]}{(2\pi\varepsilon)^{m/2}} = \frac{1}{(2\pi\varepsilon)^{m/2}} \int_{\mathcal{M}} k_\varepsilon(x, y) f(y) dV_g(y)$$

²This is similar to the operator G_ε as defined in [19, 32], but we have used a different normalization since it is more convenient for our proof.

for any $f \in L^\infty(\mathcal{M})$, and let

$$A_\varepsilon(x) := \frac{\text{vol}(\mathcal{M})\mathbb{E}\left[X_1^{(\varepsilon)}\right]}{(2\pi\varepsilon)^{m/2}} = \frac{1}{(2\pi\varepsilon)^{m/2}} \int_{\mathcal{M}} k_\varepsilon(x, y) dV_g(y).$$

The following proposition implies (21), which implies Theorem 3.1.

Proposition 3.1. *Suppose that Assumptions 1 and 2 are satisfied. Fix any $f \in C^3(\mathcal{M}) \cap L^\infty(\mathcal{M})$ and $x \in \mathcal{M}$. Then*

$$f(x)A_\varepsilon(x) - G_\varepsilon f(x) = \frac{\varepsilon}{2}\Delta_g f(x) + O(\varepsilon^{3/2}) \quad (24)$$

as $\varepsilon \rightarrow 0$.

We provide a non-asymptotic version as well to better understand the benefits of a larger ε_0 . Fix any $c \in (0, 1)$. For $x \in \mathcal{M}$, define

$$r(x) := \min\left(\varepsilon_0, c \text{inj}_{(\mathcal{M}, g)}(x)\right).$$

For $x \in \mathcal{M}$ and $R > 0$, define

$$\beta(x, R) := \inf_{\substack{y \in \mathcal{M} \\ d_g(y, x) \geq R}} d(y, x). \quad (25)$$

Since we assumed that \mathcal{M} is embedded in (X, d) , $\beta(x, R)$ is strictly positive for all $x \in \mathcal{M}$ and $R > 0$ (Lemma C.2).

Proposition 3.2. *Suppose Assumption 1 holds and that Assumption 2 holds for K, ε_0 such that $\varepsilon_0^2 < \frac{1}{2K}$. Then for any $x \in \mathcal{M}$, $f \in C^3(\mathcal{M}) \cap L^\infty(\mathcal{M})$ and $\delta > 0$, there exists a constant $C > 0$ (dependent on (\mathcal{M}, g) , x , f , δ and c , but not K or ε_0) such that*

$$\left|f(x)A_\varepsilon(x) - G_\varepsilon f(x) - \frac{\varepsilon}{2}\Delta_g f(x)\right| \leq R_1(\varepsilon) + R_2(\varepsilon) + R_3(\varepsilon), \quad (26)$$

for all $\varepsilon < \delta$, where

$$\begin{aligned} R_1(\varepsilon) &:= \frac{2\text{vol}(\mathcal{M} \setminus B_{r(x)}(x)) e^{-\frac{\beta(x, r(x))^2}{2\varepsilon}} \|f\|_\infty}{(2\pi\varepsilon)^{m/2}} \\ R_2(\varepsilon) &:= C \max(1, K)\varepsilon^{3/2} \\ R_3(\varepsilon) &:= \frac{\text{area}(\mathbb{S}^{m-1})\Delta_g f(x)}{2m} \left(\frac{\int_{r(x)}^\infty e^{-\frac{y^2}{2\varepsilon}} y^{m+1} dy}{(2\pi\varepsilon)^{m/2}} \right). \end{aligned}$$

Remark 3.2. *If Assumption 2 holds for some $K, \varepsilon_0 > 0$, then without loss of generality, we can take $\varepsilon_0^2 < \frac{1}{2K}$. We assume $\varepsilon_0^2 < \frac{1}{2K}$ for Proposition 3.2 so that we can use the following inequality in our proof:*

$$d_g^2(x, y) - d^2(x, y) < Kd_g^4(x, y) < K\varepsilon_0^2 d_g^2(x, y) < \frac{d_g^2(x, y)}{2}$$

for all $x, y \in \mathcal{M}$ such that $d_g(x, y) < \varepsilon_0$.

Remark 3.3. *For a fixed K, ε_0, x and f , taking $\varepsilon \rightarrow 0$ in Proposition 3.2 gives us Proposition 3.1, so it suffices to prove Proposition 3.2. However, if ε and ε_0 are both allowed to go to 0 and $\sqrt{\varepsilon} = \Omega(r(x))$, then*

$$\varepsilon^{m/2} R_3(\varepsilon) \asymp \int_{r(x)}^\infty e^{-\frac{y^2}{2\varepsilon}} y^{m+1} dy \gtrsim \int_{a\sqrt{\varepsilon}}^\infty e^{-\frac{y^2}{2\varepsilon}} y^{m+1} dy = \Theta\left(\varepsilon^{\frac{m+2}{2}}\right)$$

for some $a > 0$, so $R_3(\varepsilon) = \Omega(\varepsilon)$. Since $r(x) \leq \varepsilon_0$, this shows that, with our current approach, $\varepsilon = o(\varepsilon_0^2)$ is a necessary condition to obtain even an $o(\varepsilon)$ error in (24). Observe that under the setting of Theorem 3.1, since $\varepsilon_n = o\left(n^{-\frac{1}{m+2}}\right)$, we need $n = \omega\left(\varepsilon_0^{-2(m+2)}\right)$ samples to obtain $\varepsilon_n \lesssim \varepsilon_0^2$.

The proof of Proposition 3.2 is almost the same as [8, Proposition 4.4]. The error $R_1(\varepsilon)$ arises from estimating

$$f(x)A_\varepsilon(x) - G_\varepsilon f(x) = \frac{1}{(2\pi\varepsilon)^{m/2}} \int_{\mathcal{M}} k_\varepsilon(x, y)(f(x) - f(y))dV_g(y)$$

with the local integral

$$I_1(x) := \frac{1}{(2\pi\varepsilon)^{m/2}} \int_{B_{r(x)}(x)} k_\varepsilon(x, y)(f(x) - f(y))dV_g(y).$$

The error $R_2(\varepsilon)$ arises from computing $I_1(x)$ in normal coordinates and approximating it with the following integral on $T_x\mathcal{M}$:

$$I_2(x) := -\frac{1}{2(2\pi\varepsilon)^{m/2}} \int_{v \in T_x\mathcal{M}, \|v\| < r(x)} e^{-\frac{\|v\|^2}{2\varepsilon}} \text{Hess}_x f(v, v)dv.$$

Lastly, the error $R_3(\varepsilon)$ arises from approximating $I_2(x)$ with

$$-\frac{1}{2(2\pi\varepsilon)^{m/2}} \int_{v \in \mathbb{R}^m} e^{-\frac{\|v\|^2}{2\varepsilon}} \text{Hess}_x f(v, v)dv = \frac{\varepsilon}{2} \Delta_g f(x).$$

It is not surprising then that even though $R_2(\varepsilon)$ controls the asymptotics for ε , if $\varepsilon_0 < c \text{inj}_{(\mathcal{M}, g)}(x)$ (i.e., $r(x) = \varepsilon_0$), decreasing ε_0 increases $R_1(\varepsilon)$ and $R_3(\varepsilon)$. For completeness, we provide a full proof of Proposition 3.2 in Appendix A. As in [8], we can extend Theorem 3.1 to non-uniform probability distributions.

Theorem 3.2. *Suppose that Assumptions 1 and 2 are satisfied, and that x_1, \dots, x_n are drawn i.i.d. from a probability distribution μ on \mathcal{M} with a density $P \in C^3(\mathcal{M}) \cap L^\infty(\mathcal{M})$ with respect to dV_g . Fix any $f \in C^3(\mathcal{M}) \cap L^\infty(\mathcal{M})$ and $x \in \mathcal{M}$. If $\varepsilon_n = 2n^{-\frac{1}{m+2+\alpha}}$ for some $\alpha > 0$, then*

$$\frac{2}{\varepsilon_n(2\pi\varepsilon_n)^{m/2}n} L^{(\varepsilon_n, n)} f(x) \rightarrow P(x)\Delta_g f(x) - 2\langle \text{grad}_g f(x), \text{grad}_g P(x) \rangle.$$

almost surely as $n \rightarrow \infty$.

Proof. As before, define $X_j^{(\varepsilon)} := k_\varepsilon(x, x_j)$, $Y_j^{(\varepsilon)} := k_\varepsilon(x, x_j)f(x_j)$, but now suppose x_1, \dots, x_n are drawn i.i.d. from μ . By Remark 3.1, it suffices to show that

$$\lim_{n \rightarrow \infty} \frac{2\mathbb{E} \left[f(x)X_1^{(\varepsilon_n)} - Y_1^{(\varepsilon_n)} \right]}{\varepsilon_n(2\pi\varepsilon_n)^{m/2}} = P(x)\Delta_g f(x) - 2\langle \text{grad}_g f(x), \text{grad}_g P(x) \rangle. \quad (27)$$

As in [8, Section 5], (27) can be proven by applying Proposition 3.1 to $\tilde{f}(y) := P(y)(f(y) - f(x))$. \square

3.2. Sufficient conditions in terms of differentiability of d^2 . Now suppose \mathcal{M} is only a smooth oriented manifold (not necessarily equipped with a Riemannian metric) and that d is a metric on \mathcal{M} . A priori, we do not know whether there exists a Riemannian metric g on \mathcal{M} such that Assumptions 1 and 2 hold for d . In this section, we show that if d^2 is sufficiently regular around the diagonal $D_{\mathcal{M}}$ of $\mathcal{M} \times \mathcal{M}$, there exists a unique Riemannian metric on \mathcal{M} such that Assumptions 1 and 2 are satisfied.

We first recall a well-known result due to Palais [41]: a C^2 Riemannian metric g on \mathcal{M} is uniquely determined by its induced geodesic distance d_g . One way to see this (as noted in [53, p. 161]) is as follows: for any smooth path $\gamma: (-\delta, \delta) \rightarrow \mathcal{M}$, given d_g , we can recover the Riemannian metric via

$$\sqrt{\langle \gamma'(0), \gamma'(0) \rangle_{\gamma(0)}} = \lim_{t \rightarrow 0} \frac{d_g(\gamma(0), \gamma(t))}{t},$$

or equivalently,

$$\langle \gamma'(0), \gamma'(0) \rangle_{\gamma(0)} = \lim_{t \rightarrow 0} \frac{d_g^2(\gamma(0), \gamma(t))}{t^2}$$

More succinctly, if g is C^3 — which implies that \exp_x is C^2 around 0, so $d_g^2(\cdot, x)$ is C^2 around $x \in \mathcal{M}$ — we have

$$g_x = \frac{1}{2} \text{Hess}_x (d_g^2(\cdot, x))$$

for all $x \in \mathcal{M}$. Now if \mathcal{M} is a smooth manifold and d^2 is C^{k+3} on a neighborhood of the diagonal $D_{\mathcal{M}}$ of $\mathcal{M} \times \mathcal{M}$ for some $k \geq 2$, then

$$g_x = \frac{1}{2} \text{Hess}_x (d^2(\cdot, x)) \tag{28}$$

is a C^{k+1} Riemannian metric such that

$$d(x, \exp_x(tv)) = t + o(t) \tag{29}$$

for all $(x, v) \in T\mathcal{M}$ such that $g_x(v, v) = 1$, and the associated exponential map \exp is C^k on a neighborhood of $\mathcal{M} \times \{0\} \subset T\mathcal{M}$ (see Section 2.4). Suppose \tilde{g} is another C^2 Riemannian metric on \mathcal{M} , and let $d_{\tilde{g}}$ and $\widetilde{\exp}$ be the geodesic distance and the exponential map, respectively, for \tilde{g} . If \tilde{g} satisfies

$$d(x, \widetilde{\exp}_x(tv)) = t + o(t) = d_{\tilde{g}}(x, \widetilde{\exp}_x(tv)) + o(t)$$

for all $(x, v) \in T\mathcal{M}$ such that $\tilde{g}_x(v, v) = 1$, then

$$\tilde{g}_x(v, v) = \lim_{t \rightarrow 0} \frac{d_{\tilde{g}}^2(x, \widetilde{\exp}_x(tv))}{t^2} = \lim_{t \rightarrow 0} \frac{d^2(x, \widetilde{\exp}_x(tv))}{t^2} = g_x(v, v)$$

for any $(x, v) \in T\mathcal{M}$. Hence the Riemannian metric g in (28) is the unique C^2 Riemannian metric on \mathcal{M} such that (29) holds. (29) is a pointwise version of Assumption 1; for Assumption 1 to hold, we would like to bound $|d(x, \exp_x(tv)) - t|$ uniformly over all $(x, v) \in T\mathcal{M}$ such that $g_x(v, v) = 1$. It turns out that with a few additional regularity assumptions, Assumption 1 and Assumption 2 both hold.

Theorem 3.3. *Suppose d is a metric on \mathcal{M} such that d^2 is C^{k+3} on a neighborhood of $D_{\mathcal{M}}$ for some $k \geq 4$. Equip \mathcal{M} with the Riemannian metric g as defined in (28). For each $(x, v) \in T\mathcal{M}$ such that $g_x(v, v) = 1$, define*

$$h_{(x,v)}(t) := d^2(x, \exp_x(tv)) \tag{30}$$

for all t where $\exp_x(tv)$ is well-defined. Suppose moreover that there exists $\kappa, \rho > 0$ satisfying the following:

- (1) for any $x, y \in \mathcal{M}$ such that $d_g(x, y) < \rho$, there exists a length-minimizing geodesic γ from x to y such that d^2 is C^4 on $\text{Im } \gamma \times \text{Im } \gamma$;
- (2) if $|t| < \rho$, then the fourth derivative $h_{(x,v)}^{(4)}(t)$ is bounded by κ :

$$\left| h_{(x,v)}^{(4)}(t) \right| < \kappa$$

for all $(x, v) \in T\mathcal{M}$ such that $g_x(v, v) = 1$.

Then Assumption 1 holds and Assumption 2 holds for $K = \frac{\kappa}{24}$ and $\varepsilon_0 = \rho$. In addition, (28) is the unique C^2 Riemannian metric such that Assumptions 1 and 2 hold.

If \mathcal{M} is compact and d^2 is C^{k+3} on a neighborhood of $D_{\mathcal{M}}$ for some $k \geq 4$, then there always exist $\kappa, \rho > 0$ satisfying the required conditions for Theorem 3.3 (Lemma C.3).

Proof of Theorem 3.3. We have already discussed uniqueness, so it suffices to prove that Assumptions 1 and 2 hold. Fix any $x, y \in \mathcal{M}$ such that $d_g(x, y) < \rho$. Let $\gamma: I \rightarrow \mathcal{M}$ be a unit speed, length minimizing geodesic from $\gamma(0) = x$ to $\gamma(d_g(x, y)) = y$, where $I = [-\delta, d_g(x, y)]$ for some small enough $\delta > 0$. Let $v := \gamma'(0)$.

Since exp is C^k for $k \geq 4$, γ is C^k for $k \geq 4$. Since d^2 is C^4 on $\text{Im } \gamma \times \text{Im } \gamma$, the fourth derivative $h_{(x,v)}^{(4)}$ is well-defined and, by assumption, uniformly bounded by κ . In addition, we have the following Taylor expansion: for $t \in I$,

$$h_{(x,v)}(t) = t^2 + \frac{h_{(x,v)}^{(3)}(0)t^3}{6} + \frac{h_{(x,v)}^{(4)}(s)t^4}{24} \quad (31)$$

for some s between 0 and t . To prove Assumption 2 holds, we want to show that the third order term vanishes. To do this, we claim that, similar to Lemma 3.1,

$$d(\gamma(t_0), \gamma(t_1)) \leq |t_1 - t_0| = d_g(\gamma(t_0), \gamma(t_1)) \quad (32)$$

for all $t_0, t_1 \in I$. Indeed,

$$\begin{aligned} H: I \times I &\rightarrow \mathbb{R} \\ t_0, t_1 &\mapsto d^2(\gamma(t_0), \gamma(t_1)) \end{aligned}$$

is C^4 on the compact set $I \times I$. The third derivatives of H can then be uniformly bounded by some $C > 0$, so

$$\left| d^2(\gamma(t_0), \gamma(t_1)) - (t_1 - t_0)^2 \right| \leq C|t_1 - t_0|^3$$

for all $t_0, t_1 \in I$. It follows that

$$\left| d(\gamma(t_0), \gamma(t_1)) - |t_1 - t_0| \right| \leq \frac{C|t_1 - t_0|^3}{d(\gamma(t_0), \gamma(t_1)) + |t_1 - t_0|} \leq C|t_1 - t_0|^2,$$

and (32) follows from a similar argument as the proof of Lemma 3.1. Hence

$$h_{(x,v)}(t) - t^2 = d^2(\gamma(0), \gamma(t)) - t^2 \leq 0$$

for all $t \in I$, so $h_{(x,v)}^{(3)}(0)$ must be 0. Then for any $t \in I$,

$$0 \leq t^2 - h_{(x,v)}(t) \leq \left| \frac{h_{(x,v)}^{(4)}(s)t^4}{24} \right| \leq \frac{\kappa t^4}{24}$$

for some s between 0 and t . Taking $t = d_g(x, y)$ gives us

$$0 \leq d_g^2(x, y) - d^2(x, y) \leq \frac{\kappa d_g^4(x, y)}{24}$$

for any $x, y \in \mathcal{M}$ such that $d_g(x, y) < \rho$. This implies that Assumption 1 holds and that Assumption 2 holds for $K = \frac{\kappa}{24}$ and $\varepsilon_0 = \rho$. \square

We emphasize that uniqueness in Theorem 3.3 is for a given metric d : if there exist multiple distinct metrics d_1, \dots, d_k satisfying Assumptions 1 and 2, they may induce *different* Riemannian metrics g_1, \dots, g_k on \mathcal{M} , and therefore the graph Laplacian may converge to a different operator. We provide an example of this in Section 4.1. As observed in [34], the learned Riemannian metric may not agree with what the user thinks of as the “ground truth” Riemannian metric, and in general, this is unavoidable regardless of the metric we use to measure the distance between data points.

4. EXAMPLES

It follows immediately from Theorem 3.3 that Theorem 3.1 and Theorem 3.2 (pointwise convergence of graph Laplacians) applies to smooth compact submanifolds of Euclidean space and more generally, smooth compact submanifolds of a Hilbert space. This is already quite useful, since a number of metrics which have been used in data science and machine learning are Hilbertian, i.e., the associated metric space can be isometrically embedded into a Hilbert space. Examples of Hilbertian metrics include the Wasserstein-2 distance on $\mathcal{P}_2(\mathbb{R})$ [42], the sliced-Wasserstein distance [13] and the energy distance [49]³.

However, not all metrics are Hilbertian. Schoenberg’s theorem tells us that a metric space (X, d) can be isometrically embedded into a Hilbert space if and only if $y^T [d^2(x_i, x_j)]_{i,j} y \leq 0$ for all $x_1, \dots, x_n \in X$ and $y \in \mathbb{R}^n$ such that $\sum_i y_i = 0$ [45]. In fact, for $d \geq 2$, the Wasserstein-2 distance on $\mathcal{P}_2(\mathbb{R}^d)$ is not Hilbertian [42]. In this section, we provide additional examples of manifolds and metrics which satisfy the required conditions for Theorem 3.1 and Theorem 3.2.

4.1. Weighted ℓ_1 -norm. Consider the weighted ℓ_1 -norm on \mathbb{R}^2 given by

$$\|x\|_{w,1} = w_1|x_1| + w_2|x_2|$$

for some $w_1, w_2 > 0$ and the embedding

$$\begin{aligned} \iota: \mathbb{S}^1 &\rightarrow \mathbb{R}^2 \\ \theta &\mapsto (\cos \theta, \sin \theta). \end{aligned}$$

In other words, consider the following metric on \mathbb{S}^1 :

$$d(\psi, \theta) := w_1|\cos \psi - \cos \theta| + w_2|\sin \psi - \sin \theta|$$

for $\psi, \theta \in [0, 2\pi)$. Let g be the standard Riemannian metric on \mathbb{S}^1 arising from the restriction of the Euclidean metric on \mathbb{R}^2 . In [30, Section 3.7], Kileel et al. prove that if $\theta_1, \dots, \theta_n$ are drawn i.i.d.

³The energy distance between two measures μ, ν on \mathbb{R}^N is a scalar multiple of the homogeneous negative Sobolev norm $\|\mu - \nu\|_{\dot{H}^{-\frac{N+1}{2}}}$ [42, 49] and has also been called the sliced-Cramér distance [31, 39]. See also the sliced-Volterra distance [35], which is defined on integrable, compactly supported functions f, g on \mathbb{R}^N and agrees with the energy/sliced-Cramér distance if f, g are probability densities.

uniformly with respect to g , then the (appropriately scaled) graph Laplacians constructed using d converge pointwise to a scalar multiple of

$$\text{sign}(\cos \theta \sin \theta) \frac{-w_1 |\cos \theta| + w_2 |\sin \theta|}{(w_1 |\sin \theta| + w_2 |\cos \theta|)^4} \frac{d}{d\theta} + \frac{1}{3(w_1 |\sin \theta| + w_2 |\cos \theta|)^3} \frac{d^2}{d\theta^2}, \quad (33)$$

which they describe as an extrinsic operator. Here we show that we can also understand (33) as an intrinsic operator on $\mathbb{S}^1 \setminus \{0, \frac{\pi}{2}, \pi, \frac{3\pi}{2}\}$ with a different Riemannian metric and a non-uniform probability distribution.

To prove the pointwise convergence of graph Laplacians, we check that the assumptions of Theorem 3.3 hold. The key is to observe that for $(\psi, \theta) \in (0, \frac{\pi}{2})^2 \cup (\frac{\pi}{2}, \pi)^2 \cup (\pi, \frac{3\pi}{2})^2 \cup (\frac{3\pi}{2}, 2\pi)^2$,

$$\psi, \theta \mapsto d^2(\psi, \theta) = \|(\cos \psi - \cos \theta, \sin \psi - \sin \theta)\|_{w,1}^2$$

is smooth. By (28), for $\theta \in [0, 2\pi) \setminus \{0, \frac{\pi}{2}, \pi, \frac{3\pi}{2}\}$, the Riemannian metric

$$\begin{aligned} \tilde{g}_\theta \left(\frac{d}{d\theta}, \frac{d}{d\theta} \right) &:= \left(\lim_{\varepsilon \rightarrow 0} \frac{\|(\cos(\theta + \varepsilon) - \cos(\theta), \sin(\theta + \varepsilon) - \sin(\theta))\|_{w,1}}{|\varepsilon|} \right)^2 \\ &= \left(\lim_{\varepsilon \rightarrow 0} \frac{w_1 |\cos(\theta + \varepsilon) - \cos(\theta)| + w_2 |\sin(\theta + \varepsilon) - \sin(\theta)|}{|\varepsilon|} \right)^2 \\ &= (w_1 |\sin \theta| + w_2 |\cos \theta|)^2 \end{aligned}$$

provides a first-order approximation of $\|\cdot\|_{w,1}$ on $\mathbb{S}^1 \setminus \{0, \frac{\pi}{2}, \pi, \frac{3\pi}{2}\}$. Moreover, $\mathbb{S}^1 \setminus \{0, \frac{\pi}{2}, \pi, \frac{3\pi}{2}\}$ has finite volume with respect to \tilde{g} . If $\psi, \theta \in [0, 2\pi) \setminus \{0, \frac{\pi}{2}, \pi, \frac{3\pi}{2}\}$ lie in different connected components, then the geodesic distance $d_{\tilde{g}}(\psi, \theta)$ is infinite, so it suffices to check that the assumptions for Theorem 3.3 hold on each connected component. Take any $\psi \in (0, \frac{\pi}{2})$; the argument for the other quadrants is similar. Define

$$\begin{aligned} \gamma: \left(-\psi, \frac{\pi}{2} - \psi \right) &\rightarrow \left(0, \frac{\pi}{2} \right) \\ t &\mapsto \psi + t \end{aligned}$$

and its (signed) length

$$l(t) := \int_0^t \sqrt{\tilde{g}_{\gamma(\theta)} \left(\frac{d}{d\theta}, \frac{d}{d\theta} \right)} d\theta = \int_0^t w_1 \sin(\psi + \theta) + w_2 \cos(\psi + \theta) d\theta.$$

for $t \in (-\psi, \frac{\pi}{2} - \psi)$. Since l is strictly increasing and smooth, it has a smooth inverse l^{-1} . Reparametrizing γ by arc-length (with respect to \tilde{g}) gives us

$$\tilde{\gamma} := \gamma \circ l^{-1},$$

a length-minimizing unit-speed geodesic (with respect to \tilde{g}) that connects ψ to each $\theta \in (0, \frac{\pi}{2})$. Moreover, d^2 is smooth on $\text{Im } \tilde{\gamma} \times \text{Im } \tilde{\gamma} = (0, \frac{\pi}{2}) \times (0, \frac{\pi}{2})$, and its derivatives up to fourth order can be uniformly bounded in terms of w_1 and w_2 . Since the first four derivatives of l^{-1} can also be uniformly bounded in terms of w_1 and w_2 , e.g.,

$$|(l^{-1})'(s)| = \frac{1}{|w_1 \sin(\psi + l^{-1}(s)) + w_2 \cos(\psi + l^{-1}(s))|} \leq \frac{1}{\min_{\theta \in [0, \frac{\pi}{2}]} |w_1 \sin \theta + w_2 \cos \theta|}$$

for all $s \in \text{Im } l$, the fourth derivative of $h_{(\psi, \tilde{\gamma}'(0))}(t) := d^2(\psi, \tilde{\gamma}(t))$, $t \in \text{Im } l$ can be bounded in terms of w_1 and w_2 . Hence the assumptions for Theorem 3.3 hold for some $\kappa, \rho > 0$.

To identify the limiting operator, observe that the uniform distribution with respect to g is a *non-uniform* probability distribution with respect to \tilde{g} with probability density

$$P(\theta) = \frac{1}{2\pi(w_1|\sin\theta| + w_2|\cos\theta|)},$$

and by Theorem 3.2, the limiting operator of the graph Laplacians constructed with d is given by

$$P(\theta) \left(\Delta_{\tilde{g}} f(\theta) - \frac{2}{P(\theta)} \tilde{g}_\theta (\text{grad}_{\tilde{g}} f, \text{grad}_{\tilde{g}} P) \right)$$

for any $\theta \in [0, 2\pi) \setminus \{0, \frac{\pi}{2}, \pi, \frac{3\pi}{2}\}$ and smooth $f: \mathbb{S}^1 \rightarrow \mathbb{R}$. Using the formula for the Laplacian and gradient in coordinates, we have

$$\begin{aligned} \Delta_{\tilde{g}} &= -\frac{1}{w_1|\sin\theta| + w_2|\cos\theta|} \frac{d}{d\theta} \left(\frac{1}{w_1|\sin\theta| + w_2|\cos\theta|} \frac{d}{d\theta} \right) = -(2\pi)^2 P(\theta) \frac{d}{d\theta} \left(P(\theta) \frac{d}{d\theta} \right) \\ \tilde{g}_\theta (\nabla_{\tilde{g}} f, \nabla_{\tilde{g}} P) &= \tilde{g}_\theta \left(\left(\frac{1}{w_1|\sin\theta| + w_2|\cos\theta|} \right)^2 \frac{df}{d\theta} \frac{d}{d\theta}, \left(\frac{1}{w_1|\sin\theta| + w_2|\cos\theta|} \right)^2 \frac{dP}{d\theta} \frac{d}{d\theta} \right) \\ &= \left(\frac{1}{w_1|\sin\theta| + w_2|\cos\theta|} \right)^2 \frac{df}{d\theta}(\theta) \frac{dP}{d\theta}(\theta) \\ &= (2\pi)^2 P(\theta)^2 \frac{df}{d\theta}(\theta) \frac{dP}{d\theta}(\theta). \end{aligned}$$

Therefore, we obtain that the limiting operator is

$$P(\theta) \left(\Delta_{\tilde{g}} f(\theta) - \frac{2}{P(\theta)} \tilde{g}_\theta (\nabla_{\tilde{g}} f, \nabla_{\tilde{g}} P) \right) = -(2\pi)^2 \left((P(\theta))^3 \frac{d^2 f}{d\theta^2}(\theta) + 3P(\theta)^2 \frac{dP}{d\theta}(\theta) \frac{df}{d\theta}(\theta) \right),$$

which, upon computation, is a scalar multiple of (33).

4.2. Wasserstein distance. First observe that if (\mathcal{M}, g) is a smooth compact Riemannian submanifold of another smooth finite-dimensional Riemannian manifold $(\tilde{\mathcal{M}}, \tilde{g})$ with geodesic distance $d_{\tilde{g}}$, then $d_{\tilde{g}}^2$ is a C^∞ function around the diagonal of $\mathcal{M} \times \mathcal{M}$, so by Theorem 3.3, Assumptions 1 and 2 are satisfied for g and $d_{\tilde{g}}$.

As introduced in Section 2.2.1, the Wasserstein space $(\mathcal{P}_2(\mathbb{R}^N), W_2)$ is equipped with a formal Riemannian structure. For $k \in \mathbb{Z}_{\geq 0}$, if W_2^2 is C^{k+2} on a neighborhood of the diagonal of $\mathcal{M} \times \mathcal{M}$, then the Riemannian metric in (28) is precisely (a C^k representative of) the restriction of the formal Riemannian structure of $(\mathcal{P}_2(\mathbb{R}^N), W_2)$ to \mathcal{M} : for any $\gamma: (-\varepsilon, \varepsilon) \rightarrow \mathcal{M}$ and time-dependent vector field $\{v_s\}_{s \in (-\varepsilon, \varepsilon)}$ satisfying the continuity equation such that $v_s \in T_{\gamma(s)} \mathcal{P}_2(\mathbb{R}^N)$ almost everywhere, we have

$$\frac{1}{2} \text{Hess}_{\gamma(s)} (W_2^2(\cdot, \gamma(s))) (\gamma'(s), \gamma'(s)) = \lim_{t \rightarrow 0} \frac{W_2^2(\gamma(s+t), \gamma(s))}{t^2} = |\gamma'|^2(s) = \|v_s\|_{L^2(\gamma(s))}^2$$

for almost every $s \in (-\varepsilon, \varepsilon)$. As such, \mathcal{M} can be interpreted (at least formally) as a Riemannian submanifold of Wasserstein space. Compared to [28], this is a more direct generalization of manifold learning in Euclidean space.

We provide a few examples of Riemannian manifolds where Assumptions 1 and 2 are satisfied with the Wasserstein-2 distance.

Example 4.1 (Translations). This example is similar to [27, Section 3.3] and [28, Example 2.4]. Fix any $\lambda \in \mathcal{P}_2(\mathbb{R}^N)$ which is absolutely continuous with respect to the Lebesgue measure. For each $\theta \in \mathbb{R}^N$, define the translation map $T_\theta: \mathbb{R}^N \rightarrow \mathbb{R}^N$ by $T_\theta(x) = x + \theta$. Then for any $\theta, \theta' \in \mathbb{R}^N$, it is known (e.g., [27, Lemma 3.5]) that

$$W_2((T_\theta)_\# \lambda, (T_{\theta'})_\# \lambda) = |\theta - \theta'|,$$

so if we let \mathcal{M} be a compact submanifold of \mathbb{R}^N ,

$$\begin{aligned} \iota: \mathcal{M} &\rightarrow (\mathcal{P}_2(\mathbb{R}^N), W_2) \\ \theta &\mapsto (T_\theta)_\# \lambda \end{aligned}$$

satisfies Assumptions 1 and 2 with \mathcal{M} inheriting the typical Riemannian metric on \mathbb{R}^N .

Example 4.2 (Dilations). This example is similar to [27, Section 3.4] and [28, Example 2.5]. Again fix any $\lambda \in \mathcal{P}_2(\mathbb{R}^N)$ which is absolutely continuous with respect to the Lebesgue measure. For each $\theta = [\theta_j]_{j \in [N]} \in \mathbb{R}^N$ such that $\theta_j > 0$ for all $j = 1, \dots, N$, define $D_\theta: \mathbb{R}^N \rightarrow \mathbb{R}^N$ by $D_\theta(x) = [\theta_j x_j]_{j \in [N]}$. Then [27, Lemma 3.7] states that

$$W_2^2(D_\theta(\lambda), D_{\theta'}(\lambda)) = \sum_{j=1}^N |\theta_j - \theta'_j|^2 \int_{\mathbb{R}^N} |x_j|^2 d\lambda(x)$$

for any $\theta, \theta' \in \mathbb{R}^N$ such that $\theta_j, \theta'_j > 0$ for all j . Therefore, if \mathcal{M} is a compact submanifold of $\{\theta \in \mathbb{R}^N : \theta_j > 0 \forall j\}$,

$$\begin{aligned} \iota: \mathcal{M} &\rightarrow (\mathcal{P}_2(\mathbb{R}^N), W_2) \\ \theta &\mapsto (D_\theta)_\# \lambda \end{aligned}$$

satisfies Assumptions 1 and 2, but with \mathcal{M} equipped with the Riemannian metric

$$g\left(\frac{\partial}{\partial x^i}, \frac{\partial}{\partial x^j}\right) = \delta_{ij} \int_{\mathbb{R}^N} |x_j|^2 d\lambda(x)$$

defined on \mathbb{R}^N . (Here $\{\frac{\partial}{\partial x^j}\}_{j \in [N]}$ are the standard coordinate vectors on \mathbb{R}^N .)

Remark 4.1. For convenience, we have taken \mathcal{M} to be a smooth manifold in this paper, though Example 4.1 and Example 4.2 also work if \mathcal{M} is a compact convex subset of \mathbb{R}^N , as in [28, Example 2.4 and 2.5]. If x belongs to the interior of \mathcal{M} , then Theorem 3.1 and Theorem 3.2 also hold, following almost the same proof.

Example 4.3 (Submanifolds of the Bures-Wasserstein manifold). For a fixed $N \in \mathbb{N}$, the Bures-Wasserstein manifold — the space of non-degenerate N -dimensional Gaussians with the Riemannian structure of Wasserstein-2 space — is a finite-dimensional smooth Riemannian manifold (not just formal) [18]. Hence, by Theorem 3.3, if \mathcal{M} is a compact Riemannian submanifold of the Bures-Wasserstein manifold, Assumptions 1 and 2 are satisfied.

Additionally, in the case $N = 1$, $(\mathcal{P}_2(\mathbb{R}), W_2)$ is Hilbertian.

4.3. The rotating ball (non-)example. We warn that an embedding $\iota: \mathcal{M} \rightarrow X$ will not always satisfy Assumptions 1 and 2, even when \mathcal{M} is compact and the ambient space (X, d) is a Hilbert space. More specifically, if ι is not smooth, then we cannot view \mathcal{M} as a smooth submanifold of a Hilbert space and apply Theorem 3.3. In fact, the embedding given in the introduction

$$\begin{aligned} \iota: \mathbb{S}^1 &\rightarrow L^2(\mathbb{R}^2) \\ \theta &\mapsto \frac{1}{\pi r^2} \mathbf{1}_{B_r((\cos \theta, \sin \theta))}, \end{aligned}$$

where $r \in (0, 1]$ is fixed, is an example of this. Let (\mathcal{M}, g) be \mathbb{S}^1 with its standard Riemannian metric. Consider a ball B_1 of radius r centered at $(1, 0)$ and another ball B_2 of radius r centered at $(\cos \theta, \sin \theta)$. For small enough $\theta > 0$, the area of $B_1 \cap B_2$ can be computed via

$$\begin{aligned} \text{area}(B_1 \cap B_2) &= 2 \left(r^2 \arccos \left(\frac{\sin(\frac{\theta}{2})}{r} \right) - \sin \left(\frac{\theta}{2} \right) \sqrt{r^2 - \sin^2 \left(\frac{\theta}{2} \right)} \right) \\ &= 2 \left(r^2 \left(\frac{\pi}{2} - \frac{\sin(\frac{\theta}{2})}{r} + O \left(\left(\frac{\sin(\frac{\theta}{2})}{r} \right)^3 \right) \right) - \sin \left(\frac{\theta}{2} \right) \sqrt{r^2 - \sin^2 \left(\frac{\theta}{2} \right)} \right) \\ &= \pi r^2 - 2r\theta + O(\theta^3), \end{aligned}$$

from which it follows that

$$\|\iota(\theta) - \iota(0)\|_{L^2}^2 = 2 \left(\frac{1}{\pi r^2} \right)^2 (\pi r^2 - \text{area}(B_1 \cap B_2)) = \Theta(\theta),$$

so $\|\iota(\theta) - \iota(0)\|_{L^2} = \Theta(\sqrt{\theta})$ cannot possibly satisfy Assumption 1. In contrast, the Wasserstein-2 distance

$$W_2^2(\iota(\theta), \iota(\varphi)) = |(\cos \theta, \sin \theta) - (\cos \varphi, \sin \varphi)|^2,$$

satisfies both Assumption 1 and 2; this is equivalent to considering the typical embedding of \mathbb{S}^1 as a unit circle in \mathbb{R}^2 . Perhaps a bit less obvious is that the $L^1(\mathbb{R}^2)$ norm satisfies both Assumption 1 and 2 (with respect to a scalar multiple of g):

$$\|\iota(\theta) - \iota(0)\|_{L^1} = \frac{2}{\pi r^2} (\pi r^2 - \text{area}(B_1 \cap B_2)) = \frac{2}{\pi r^2} (2r\theta + O(\theta^3)),$$

so there exists $K, \varepsilon_0 > 0$ such that

$$\left| \|\iota(\theta) - \iota(0)\|_{L^1} - \frac{4|\theta|}{\pi r} \right| < K|\theta|^3$$

for all $|\theta| < \varepsilon_0$, which implies that there exists $\tilde{K}, \tilde{\varepsilon}_0 > 0$ such that

$$\|\iota(\theta) - \iota(0)\|_{L^1}^2 - \left(\frac{4|\theta|}{\pi r} \right)^2 = \left(\|\iota(\theta) - \iota(0)\|_{L^1} - \frac{4|\theta|}{\pi r} \right) \left(\|\iota(\theta) - \iota(0)\|_{L^1} + \frac{4|\theta|}{\pi r} \right) \leq \tilde{K}|\theta|^4$$

for all $|\theta| < \tilde{\varepsilon}_0$.

Remark 4.2. *Since*

$$\|\iota(\theta) - \iota(0)\|_{L^1} = \pi r^2 \|\iota(\theta) - \iota(0)\|_{L^2}^2,$$

applying the Laplacian eigenmaps algorithm with the $L^2(\mathbb{R}^2)$ norm and Gaussian kernel is equivalent to applying the Laplacian eigenmaps algorithm with the $L^1(\mathbb{R}^2)$ norm and Laplace kernel

$$\tilde{k}_\beta(x, y) := e^{-\frac{d(x, y)}{2\beta}}$$

with $\beta = \pi r^2 \varepsilon$. We leave the study of the convergence of the graph Laplacians with other kernels to future work, though our numerical experiments in Section 5 suggest that the Gaussian kernel exhibits better performance with graph Laplacian-based methods.

5. NUMERICAL EXPERIMENTS

In this section, we demonstrate the convergence of the graph Laplacian in Theorem 3.1 with numerical experiments, using the rotating ball example from Section 4.3. For all experiments, we discretize $[-2, 2] \times [-2, 2]$ into images of size 128×128 and take (\mathcal{M}, g) to be \mathbb{S}^1 with its standard Riemannian metric. Additionally, for convenience, we use the embeddings

$$\begin{aligned} \iota_r : \mathbb{S}^1 &\rightarrow L^2\left(\overline{B_2(0)}\right) \\ \theta &\mapsto \frac{1}{4r} \mathbf{1}_{B_r((\cos \theta, \sin \theta))} \end{aligned}$$

instead of the normalization in (1) so that by our calculations in Section 4.3, the $L^1(\mathbb{R}^2)$ norm $\theta, \varphi \mapsto \|\iota_r(\theta) - \iota_r(\varphi)\|_{L^1}$ approximates the geodesic distance d_g on (\mathcal{M}, g) for all $r \in (0, 1]$. We confirm this in Fig. 4. We test pointwise convergence on $f(\theta) := \sin(\theta)$, whose Laplacian can be explicitly computed as $\Delta_g f(\theta) = \sin(\theta)$ for all $\theta \in [0, 2\pi)$. Each graph Laplacian constructed from n samples is multiplied by $\frac{4\pi}{\varepsilon_n(2\pi\varepsilon_n)^{1/2}n}$, where $\varepsilon_n = 2n^{-\frac{1}{m+2+\alpha}}$ and $\alpha = 0.01$, so that if the assumptions of Theorem 3.1 are satisfied, the pointwise (almost everywhere) limit should be $\Delta_g f$. The code to reproduce the results in this section can be found at https://github.com/lzx23/manifold_learning_metric_spaces.

5.1. Comparison of different metrics. For this experiment, we fix $r = 0.75$. We compare several different metrics which we have already discussed:

- **$L^1(\mathbb{R}^2)$ norm:** as discussed in Section 4.3,

$$d(\theta, \varphi) = \|\iota_r(\theta) - \iota_r(\varphi)\|_{L^1}$$

locally approximates the geodesic distance on \mathcal{M} with the standard metric.

- **$L^2(\mathbb{R}^2)$ norm:** for our experiments, this refers to the metric induced by the $L^2(\mathbb{R}^2)$ norm with the following normalization:

$$d(\theta, \varphi) = \sqrt{4r} \|\iota_r(\theta) - \iota_r(\varphi)\|_{L^2}.$$

This normalization satisfies

$$\left(\sqrt{4r} \|\iota_r(\theta) - \iota_r(\varphi)\|_{L^2(\mathbb{R}^2)}\right)^2 = \|\iota_r(\theta) - \iota_r(\varphi)\|_{L^1(\mathbb{R}^2)}$$

for all $\theta, \varphi \in \mathbb{S}^1$, which allows us to simultaneously investigate the effect of using a Laplace kernel instead of a Gaussian kernel (see Remark 4.2).

- **\mathbb{R}^2 norm:** this refers to the metric

$$d(\theta, \varphi) = |(\cos \theta, \sin \theta) - (\cos \varphi, \sin \varphi)|.$$

As discussed in the introduction, if $\iota_r(\theta)$ is normalized to be a probability density for all $\theta \in \mathbb{S}^1$, this agrees with the Wasserstein-2 metric.

In Fig. 1, we plot $\theta \mapsto d(\theta, 0)$ for each of the aforementioned metrics. We also include the geodesic distance $d_g(\theta, 0) = |\theta|$ for comparison. Fig. 1 confirms our calculations in Section 4.3: the $L^1(\mathbb{R}^2)$ norm approximates $d_g(\theta, 0) = |\theta|$ around 0, whereas the $L^2(\mathbb{R}^2)$ norm behaves like $\sqrt{|\theta|}$ around 0.

Although the $L^1(\mathbb{R}^2)$ and \mathbb{R}^2 norm both approximate the geodesic distance d_g around 0, Fig. 1 suggests that the \mathbb{R}^2 norm provides a better approximation. In Fig. 2, we draw n samples $\theta_1, \dots, \theta_n$

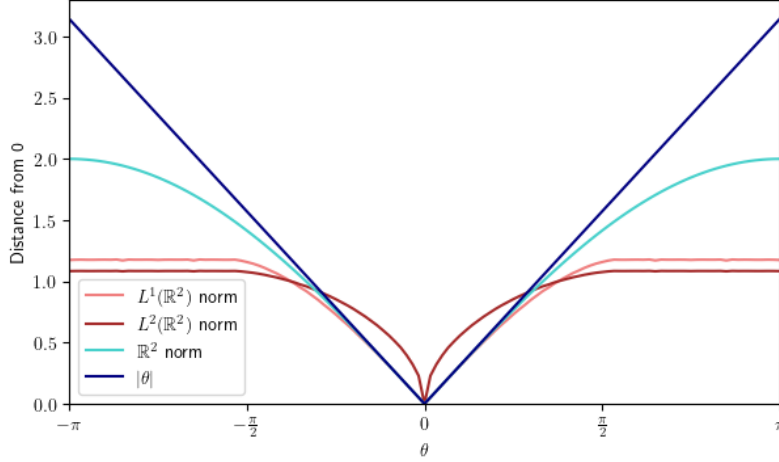


FIGURE 1. Comparison of different metrics.

i.i.d. from the uniform distribution on (\mathcal{M}, g) and plot the discrete Laplacian of f constructed with each of the metrics in Fig. 1 (and the Gaussian kernel). We see that the discrete Laplacian with the \mathbb{R}^2 norm converges to $\Delta_g f$ much faster than the discrete Laplacian with $L^1(\mathbb{R}^2)$ norm, whereas the discrete Laplacian with the $L^2(\mathbb{R}^2)$ norm (equivalently, the discrete Laplacian with a Laplace kernel and $L^1(\mathbb{R}^2)$ norm) does not converge to $\Delta_g f$.

Although we did not study spectral convergence in this work, we are ultimately motivated by the use of various metrics in the Laplacian eigenmaps and diffusion maps algorithms. Therefore, we also plot the embeddings obtained from the first two non-trivial eigenvectors of the normalized graph Laplacian in Fig. 3. Again we see that using metrics which better approximate d_g results in embeddings which better capture the geometry of (\mathcal{M}, g) , especially at lower sample sizes.

5.2. Changing radii. To obtain finer control over the quality of the approximation of d_g , we now consider varying the radius r of our rotating ball. Indeed, we have the following lemma.

Lemma 5.1. *If $0 < r_1 < r_2 \leq 1$, then $\|\iota_{r_1}(\theta) - \iota_{r_1}(0)\|_{L^1} \leq \|\iota_{r_2}(\theta) - \iota_{r_2}(0)\|_{L^1}$ for any $\theta \in [-\pi, \pi]$, and the inequality is strict for $\theta \neq 0$.*

We prove Lemma 5.1 in Appendix B. As a direct corollary, if $r_1 < r_2$, then $\|\iota_{r_2}(\theta) - \iota_{r_2}(0)\|_{L^1}$ is a better approximation of $d_g(\theta, 0) = |\theta|$ than $\|\iota_{r_1}(\theta) - \iota_{r_1}(0)\|_{L^1}$ in the following sense:

Corollary 5.1.1. *Suppose $0 < r_1 < r_2 \leq 1$, and that $\theta, \varphi \mapsto \|\iota_{r_1}(\theta) - \iota_{r_1}(\varphi)\|_{L^1}^2$ satisfies Assumption 2 for some $K, \varepsilon_0 > 0$, i.e.,*

$$|\theta|^2 - \|\iota_{r_1}(\theta) - \iota_{r_1}(0)\|_{L^1}^2 < K|\theta|^4$$

for all $|\theta| < \varepsilon_0$. Then there exists $\tilde{\varepsilon}_0 > \varepsilon_0$ such that

$$|\theta|^2 - \|\iota_{r_2}(\theta) - \iota_{r_2}(0)\|_{L^1}^2 < K|\theta|^4$$

for all $|\theta| < \tilde{\varepsilon}_0$.

Proof. This follows from Lemma 5.1 and the fact that $\theta \mapsto \|\iota_r(\theta) - \iota_r(0)\|_{L^1}^2$ is continuous for any fixed r . \square

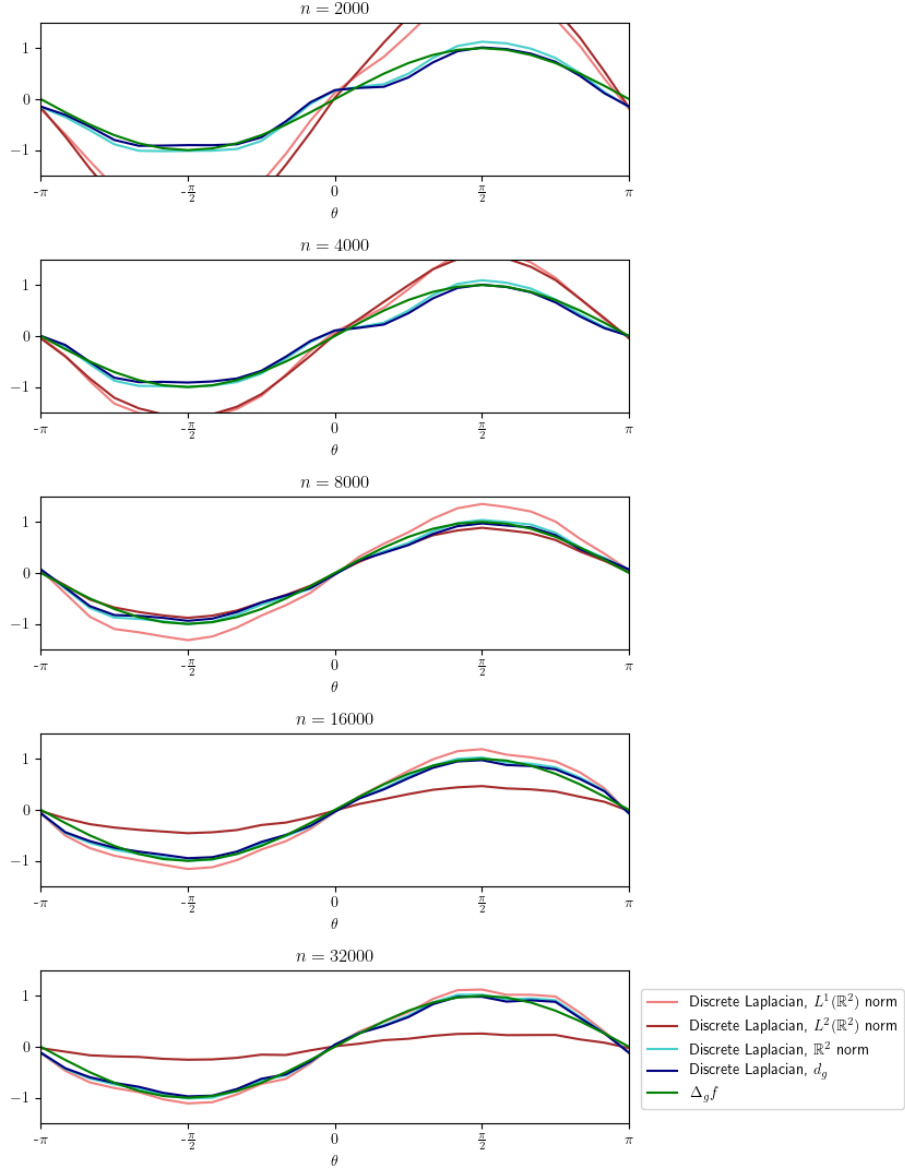


FIGURE 2. Comparison of the discrete Laplacian for different metrics.

We confirm in Fig. 4 that the $L^1(\mathbb{R}^2)$ norm $\|\iota_r(\theta) - \iota_r(0)\|_{L^1}$ locally approximates the geodesic distance $d_g(\theta, 0) = |\theta|$ for each r , but that larger r result in better approximations.

As in Section 5.1, we draw $\theta_1, \dots, \theta_n$ i.i.d. from the uniform distribution on (\mathcal{M}, g) . We compare the resulting discrete Laplacians in Fig. 5 and see that a larger radius r , which gives us a better approximation of d_g , also results in faster convergence of the discrete Laplacians. Similarly, in

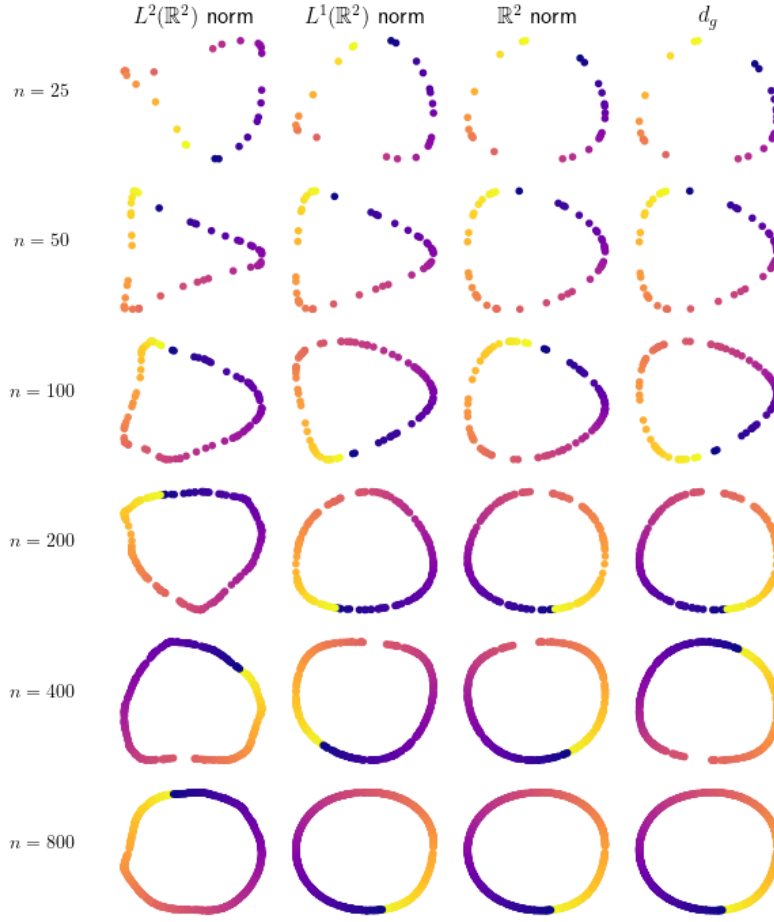


FIGURE 3. Laplacian eigenmap embeddings using the first two non-trivial eigenvectors $v^{(1)}, v^{(2)}$ of the normalized graph Laplacian $\mathcal{L}^{(\varepsilon_n, n)}$ constructed with different metrics. More specifically, $\theta_1, \dots, \theta_n$ are once again drawn i.i.d. from the uniform distribution on \mathbb{S}^1 . The first two non-trivial eigenvectors $v^{(1)}, v^{(2)}$ of $\mathcal{L}^{(\varepsilon_n, n)}$ with the specified metric are computed, and each sample θ_i is mapped to $\left(v_i^{(1)}, v_i^{(2)}\right)$ and colored by the true angle θ_i .

Fig. 6, we observe that the Laplacian eigenmap embeddings capture the geometry of (\mathcal{M}, g) much better for larger r , and this effect is most pronounced for lower sample sizes.

6. CONCLUSION

In this paper, we provided sufficient conditions for the pointwise convergence of graph Laplacians when a manifold \mathcal{M} is embedded in a metric space (X, d) . Moreover, we showed that if \mathcal{M} is compact and d^2 has enough regularity around the diagonal of $\mathcal{M} \times \mathcal{M}$, then there exists a unique Riemannian metric g on \mathcal{M} such that the graph Laplacians converge pointwise to the Laplace-Beltrami operator

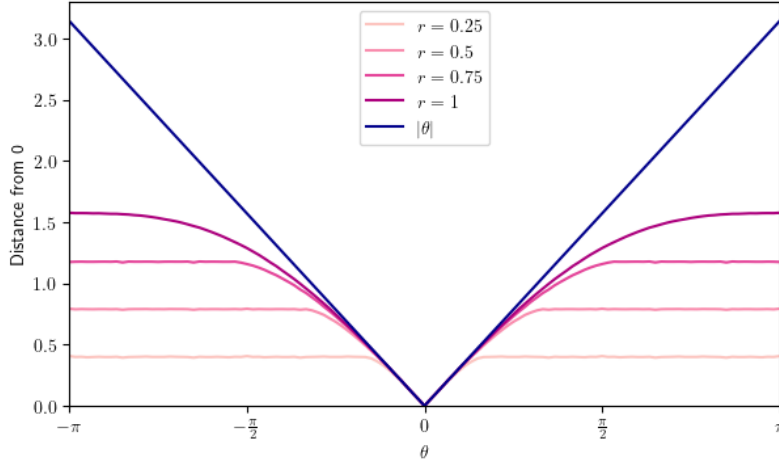


FIGURE 4. The L^1 norm $\|\iota_r(\theta) - \iota_r(0)\|_{L^1}$ with balls of varying radii r .

Δ_g on (\mathcal{M}, g) . We also included non-asymptotic upper bounds on the bias error and demonstrated numerically that due to limited sample sizes, the choice of metric can have a sizable impact on the convergence of graph Laplacians in practice.

Our work suggests several directions for future research. One direction would be to generalize other results from the Euclidean case, e.g., [14, 15, 16, 17, 17, 19, 20, 25, 25, 29, 51]. Of particular interest for manifold learning is obtaining non-asymptotic bounds for spectral convergence similar to Proposition 3.2 and determining whether they are tight. Another direction would be to study the stability of the Laplacian eigenmap embedding if we use an approximation of the metric d instead of d itself in the graph Laplacian. For example, in practice, it may be preferable to use an entropy-regularized approximation of the Wasserstein distance [22] or a linearization of the Wasserstein-2 distance [26, 36, 54], since computing the pairwise Wasserstein-2 distance between many measures can be computationally expensive. Lastly, for an embedding $\iota: \mathcal{M} \rightarrow (\mathcal{P}_2(\mathbb{R}^N), W_2)$, it would be of interest to characterize when W_2^2 is regular around the diagonal of $\mathcal{M} \times \mathcal{M}$ and to better understand whether this is a good assumption for various practical applications.

ACKNOWLEDGMENTS

A.S. and L.X. were supported in part by AFOSR FA9550-23-1-0249, the Simons Foundation Math+X Investigator Award, NSF DMS 2009753, and NIH/NIGMS R01GM136780-01. L.X. was supported in part by NSF Graduate Research Fellowship DGE-2039656. Any opinions, findings, and conclusions or recommendations expressed in this material are those of the authors and do not necessarily reflect the views of the National Science Foundation. We thank Ruiyi Yang and Roy Lederman for helpful discussions.

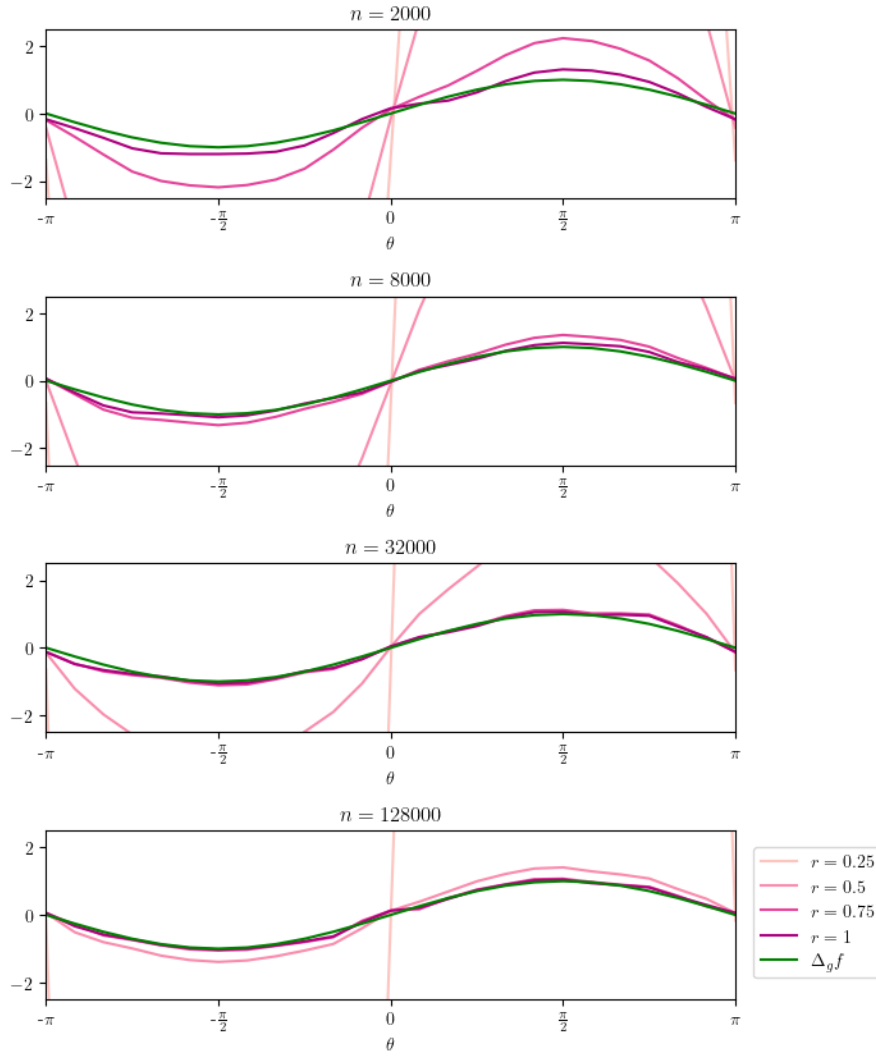


FIGURE 5. Comparison of the discrete Laplacian with the metric induced by the L^1 norm $\theta, \varphi \mapsto \|\iota_r(\theta) - \iota_r(\varphi)\|_{L^1}$ for different values of r .

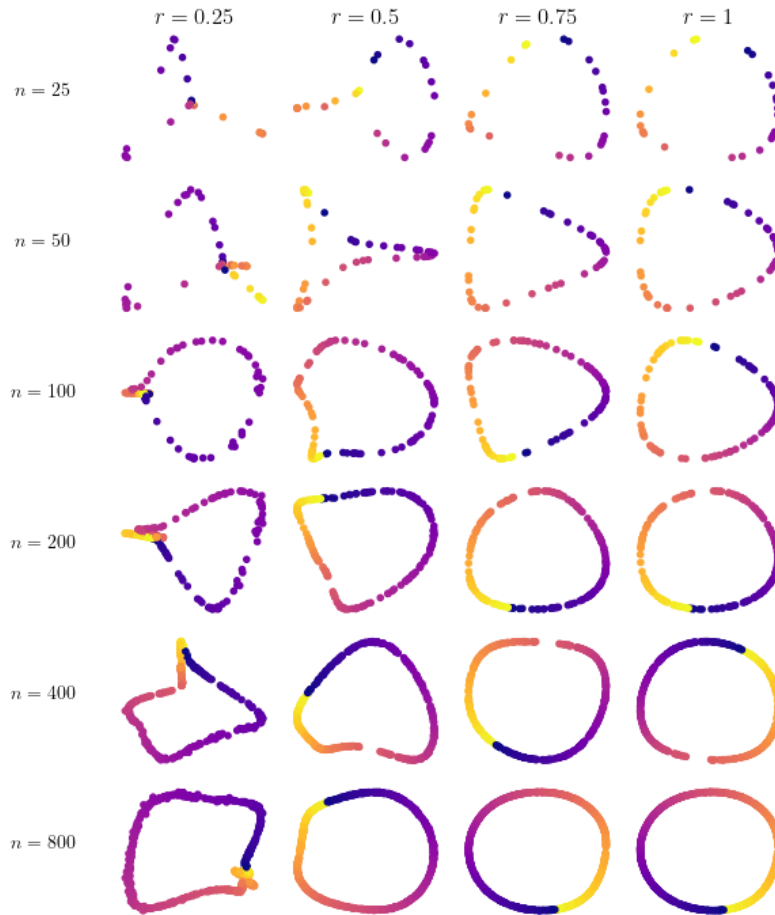


FIGURE 6. Laplacian eigenmaps embedding, again using the first two non-trivial eigenvectors of the normalized graph Laplacian $\mathcal{L}^{(\varepsilon_n, n)}$. The procedure is the same as Fig. 3, except that we use the metrics $\theta, \varphi \mapsto \|\iota_r(\theta) - \iota_r(\varphi)\|_{L^1}$ for $r = 0.25, 0.5, 0.75, 1$.

REFERENCES

- [1] H. Abdalla. Embedding Riemannian manifolds via their eigenfunctions and their heat kernel. *Bulletin of the Korean Mathematical Society*, 49(5):939–947, 2012.
- [2] L. Ambrosio, N. Gigli, and G. Savaré. *Gradient flows: in metric spaces and in the space of probability measures*. Springer Science & Business Media, 2008.
- [3] J. Bates. The embedding dimension of Laplacian eigenfunction maps. *Applied and Computational Harmonic Analysis*, 37(3):516–530, 2014.
- [4] M. Belkin and P. Niyogi. Laplacian eigenmaps and spectral techniques for embedding and clustering. *Advances in neural information processing systems*, 14, 2001.
- [5] M. Belkin and P. Niyogi. Laplacian eigenmaps for dimensionality reduction and data representation. *Neural computation*, 15(6):1373–1396, 2003.
- [6] M. Belkin and P. Niyogi. Towards a theoretical foundation for Laplacian-based manifold methods. In *International Conference on Computational Learning Theory*, pages 486–500. Springer, 2005.
- [7] M. Belkin and P. Niyogi. Convergence of Laplacian eigenmaps. *Advances in neural information processing systems*, 19, 2006.
- [8] M. Belkin and P. Niyogi. Towards a theoretical foundation for Laplacian-based manifold methods. *Journal of Computer and System Sciences*, 74(8):1289–1308, 2008.
- [9] P. Bérard. Volume des ensembles nodaux des fonctions propres du laplacien. *Séminaire de théorie spectrale et géométrie*, 3:1–9, 1985.
- [10] P. Bérard, G. Besson, and S. Gallot. Embedding Riemannian manifolds by their heat kernel. *Geometric & Functional Analysis GAFA*, 4:373–398, 1994.
- [11] T. Berry and J. Harlim. Variable bandwidth diffusion kernels. *Applied and Computational Harmonic Analysis*, 40(1):68–96, 2016.
- [12] J. Bigot, R. Gouet, T. Klein, and A. Lopez. Geodesic PCA in the Wasserstein space by convex PCA. In *Annales de l’Institut Henri Poincaré (B) Probabilités et Statistiques*, volume 53, pages 1–26, 2017.
- [13] N. Bonneel, J. Rabin, G. Peyré, and H. Pfister. Sliced and Radon Wasserstein Barycenters of Measures. *Journal of Mathematical Imaging and Vision*, 51:22–45, 2015.
- [14] J. Calder and N. G. Trillos. Improved spectral convergence rates for graph Laplacians on ε -graphs and k-nn graphs. *Applied and Computational Harmonic Analysis*, 60:123–175, 2022.
- [15] X. Cheng and B. Landa. Bi-stochastically normalized graph Laplacian: convergence to manifold Laplacian and robustness to outlier noise. *Information and Inference: A Journal of the IMA*, 13(4):iaae026, 2024.
- [16] X. Cheng and H.-T. Wu. Convergence of graph Laplacian with kNN self-tuned kernels. *Inf. Inference*, 11(3):889–957, 2022.
- [17] X. Cheng and N. Wu. Eigen-convergence of Gaussian kernelized graph Laplacian by manifold heat interpolation. *Applied and Computational Harmonic Analysis*, 61:132–190, 2022.
- [18] S. Chewi, J. Niles-Weed, and P. Rigollet. Statistical optimal transport, 2024.
- [19] R. R. Coifman and S. Lafon. Diffusion maps. *Applied and computational harmonic analysis*, 21(1):5–30, 2006.
- [20] R. R. Coifman, S. Lafon, A. B. Lee, M. Maggioni, B. Nadler, F. Warner, and S. W. Zucker. Geometric diffusions as a tool for harmonic analysis and structure definition of data: Diffusion maps. *Proceedings of the national academy of sciences*, 102(21):7426–7431, 2005.
- [21] A. Collas, T. Vayer, R. Flamary, and A. Breloy. Entropic Wasserstein component analysis. In *2023 IEEE 33rd International Workshop on Machine Learning for Signal Processing (MLSP)*,

- pages 1–6. IEEE, 2023.
- [22] M. Cuturi. Sinkhorn distances: Lightspeed computation of optimal transport. *Advances in neural information processing systems*, 26, 2013.
 - [23] M. P. Do Carmo and J. Flaherty Francis. *Riemannian geometry*, volume 2. Springer, 1992.
 - [24] R. Flamary, M. Cuturi, N. Courty, and A. Rakotomamonjy. Wasserstein discriminant analysis. *Machine Learning*, 107:1923–1945, 2018.
 - [25] N. García Trillos, M. Gerlach, M. Hein, and D. Slepčev. Error estimates for spectral convergence of the graph Laplacian on random geometric graphs toward the Laplace–Beltrami operator. *Foundations of Computational Mathematics*, 20(4):827–887, 2020.
 - [26] P. Greengard, J. G. Hoskins, N. F. Marshall, and A. Singer. On a linearization of quadratic Wasserstein distance. *arXiv preprint arXiv:2201.13386*, 2022.
 - [27] K. Hamm, N. Henscheid, and S. Kang. Wassmap: Wasserstein isometric mapping for image manifold learning. *SIAM Journal on Mathematics of Data Science*, 5(2):475–501, 2023.
 - [28] K. Hamm, C. Moosmüller, B. Schmitzer, and M. Thorpe. Manifold learning in Wasserstein space, 2024.
 - [29] M. Hein, J.-Y. Audibert, and U. Von Luxburg. From graphs to manifolds—weak and strong pointwise consistency of graph Laplacians. In *International Conference on Computational Learning Theory*, pages 470–485. Springer, 2005.
 - [30] J. Kileel, A. Moscovich, N. Zelesko, and A. Singer. Manifold learning with arbitrary norms. *Journal of Fourier Analysis and Applications*, 27(5):82, 2021.
 - [31] S. Kolouri, N. A. Ketz, A. Soltoggio, and P. K. Pilly. Sliced Cramer synaptic consolidation for Preserving Deeply Learned Representations. In *International Conference on Learning Representations*, 2020.
 - [32] S. S. Lafon. *Diffusion maps and geometric harmonics*. Yale University, 2004.
 - [33] C. Lange. Regularity of the geodesic flow on submanifolds, 2024.
 - [34] R. R. Lederman and B. Toader. On manifold learning in Plato’s cave: Remarks on manifold learning and physical phenomena. In *2023 International Conference on Sampling Theory and Applications (SampTA)*, pages 1–7. IEEE, 2023.
 - [35] W. Leeb. On metrics robust to noise and deformations, 2024.
 - [36] C. Letrouit and Q. Mérigot. Gluing methods for quantitative stability of optimal transport maps. *arXiv preprint arXiv:2411.04908*, 2024.
 - [37] P. Y. Lu, R. Dangovski, and M. Soljačić. Discovering conservation laws using optimal transport and manifold learning. *Nature Communications*, 14(1):4744, 2023.
 - [38] G. Mishne, R. Talmon, R. Meir, J. Schiller, M. Lavzin, U. Dubin, and R. R. Coifman. Hierarchical coupled-geometry analysis for neuronal structure and activity pattern discovery. *IEEE Journal of Selected Topics in Signal Processing*, 10(7):1238–1253, 2016.
 - [39] K. Nadjahi, A. Durmus, L. Chizat, S. Kolouri, S. Shahrampour, and U. Simsekli. Statistical and topological properties of sliced probability divergences. *Advances in Neural Information Processing Systems*, 33:20802–20812, 2020.
 - [40] B. Nadler, S. Lafon, R. R. Coifman, and I. G. Kevrekidis. Diffusion maps, spectral clustering and reaction coordinates of dynamical systems. *Applied and Computational Harmonic Analysis*, 21(1):113–127, 2006.
 - [41] R. S. Palais. On the differentiability of isometries. *Proceedings of the American Mathematical Society*, 8(4):805–807, 1957.
 - [42] G. Peyré, M. Cuturi, et al. Computational optimal transport: With applications to data science. *Foundations and Trends® in Machine Learning*, 11(5-6):355–607, 2019.

- [43] S. Rosenberg. *The Laplacian on a Riemannian manifold: an introduction to analysis on manifolds*. Number 31. Cambridge University Press, 1997.
- [44] F. Santambrogio. *Optimal transport for applied mathematicians*, volume 87 of *Progress in Nonlinear Differential Equations and their Applications*. Birkhäuser/Springer, Cham, 2015. Calculus of variations, PDEs, and modeling.
- [45] I. J. Schoenberg. Metric spaces and positive definite functions. *Transactions of the American Mathematical Society*, 44(3):522–536, 1938.
- [46] V. Seguy and M. Cuturi. Principal geodesic analysis for probability measures under the optimal transport metric. *Advances in Neural Information Processing Systems*, 28, 2015.
- [47] S. Shirdhonkar and D. W. Jacobs. Approximate earth mover’s distance in linear time. In *2008 IEEE Conference on Computer Vision and Pattern Recognition*, pages 1–8. IEEE, 2008.
- [48] A. Singer. From graph to manifold Laplacian: The convergence rate. *Applied and Computational Harmonic Analysis*, 21(1):128–134, 2006.
- [49] G. J. Székely. E-statistics: The energy of statistical samples. *Bowling Green State University, Department of Mathematics and Statistics Technical Report*, 3(05):1–18, 2003.
- [50] J. B. Tenenbaum, V. d. Silva, and J. C. Langford. A global geometric framework for nonlinear dimensionality reduction. *science*, 290(5500):2319–2323, 2000.
- [51] D. Ting, L. Huang, and M. I. Jordan. An analysis of the convergence of graph Laplacians. In *Proceedings of the 27th International Conference on International Conference on Machine Learning*, pages 1079–1086, 2010.
- [52] C. Villani. *Topics in optimal transportation*, volume 58. American Mathematical Soc., 2021.
- [53] C. Villani et al. *Optimal transport: old and new*, volume 338. Springer, 2009.
- [54] W. Wang, D. Slepčev, S. Basu, J. A. Ozolek, and G. K. Rohde. A linear optimal transportation framework for quantifying and visualizing variations in sets of images. *International journal of computer vision*, 101:254–269, 2013.
- [55] N. Zelesko, A. Moscovich, J. Kileel, and A. Singer. Earthmover-based manifold learning for analyzing molecular conformation spaces. In *2020 IEEE 17th International Symposium on Biomedical Imaging (ISBI)*, pages 1715–1719. IEEE, 2020.

APPENDIX A. PROOF OF PROPOSITION 3.2

Proof of Proposition 3.2. For this proof, when \lesssim and big-O notation are used, the multiplicative constant can depend on (\mathcal{M}, g) , x , f , δ and c , but not K and ε_0 . The proof is almost the same as [8].

1. Approximation of integrals on \mathcal{M} by an integral over a geodesic ball. We first approximate $f(x)A_\varepsilon(x) - G_\varepsilon f(x)$ with the integral

$$I_1(x) := \frac{1}{(2\pi\varepsilon)^{m/2}} \int_{B_{r(x)}(x)} k_\varepsilon(x, y)(f(x) - f(y))dV_g(y).$$

This gives us an approximation error of

$$\begin{aligned} \left| f(x)A_\varepsilon(x) - G_\varepsilon f(x) - I_1(x) \right| &= \frac{1}{(2\pi\varepsilon)^{m/2}} \left| \int_{\mathcal{M} \setminus B_{r(x)}(x)} k_\varepsilon(x, y)(f(x) - f(y)) dV_g(y) \right| \\ &\leq \frac{2\text{vol}(\mathcal{M} \setminus B_{r(x)}(x)) e^{-\frac{\beta(x, r(x))^2}{2\varepsilon}} \|f\|_\infty}{(2\pi\varepsilon)^{m/2}}. \end{aligned}$$

The right-hand side is precisely $R_1(\varepsilon)$.

2. Integrate in normal coordinates. Since $r(x) < \text{inj}_{(\mathcal{M}, g)}(x)$, we can evaluate $I_1(x)$ in normal coordinates:

$$I_1(x) = \frac{1}{(2\pi\varepsilon)^{m/2}} \int_{\|v\| < r(x)} k_\varepsilon(x, \exp_x(v))(f(x) - f(\exp_x(v))) \sqrt{|\det[g(v)]|} dv.$$

We would like to approximate the integral on the right hand side with

$$I_2(x) := -\frac{1}{2(2\pi\varepsilon)^{m/2}} \int_{\|v\| < r(x)} e^{-\frac{\|v\|^2}{2\varepsilon}} \text{Hess}_x f(v, v) dv.$$

Recall that we assumed that the Riemannian metric g is C^{k+1} for $k \geq 3$, and since $r(x) \leq c \text{inj}_{(\mathcal{M}, g)}(x) < \text{inj}_{(\mathcal{M}, g)}(x)$, the exponential map \exp belongs to $C^k(\overline{B_{r(x)}(x)})$ for $k \geq 3$. Since $f \in C^3(\mathcal{M})$, we can use the Taylor expansions

$$f(\exp_x(v)) - f(x) = \langle \text{grad} f(x), v \rangle + \frac{1}{2} \text{Hess}_x f(v, v) + O(\|v\|^3) \quad (34)$$

$$\sqrt{|\det[g(v)]|} = 1 - \frac{\text{Ric}_x(v, v)}{6} + O(\|v\|^3) \quad (35)$$

on $B_{r(x)}(x)$, where Ric_x denotes the Ricci curvature tensor at x . Moreover, by Assumption 2,

$$e^{-\frac{\|v\|^2}{2\varepsilon}} \leq k_\varepsilon(x, \exp_x(v)) \leq e^{-\frac{\|v\|^2}{2\varepsilon}} e^{\frac{K\|v\|^4}{2\varepsilon}}$$

for all $v \in T_x \mathcal{M}$ such that $\|v\| < \varepsilon_0$. By the mean value theorem and convexity of the exponential function,

$$e^t \leq 1 + te^t$$

for all $t > 0$, so for all $\|v\| < \varepsilon_0$,

$$e^{\frac{K\|v\|^4}{2\varepsilon}} \leq 1 + \left(\frac{K\|v\|^4}{2\varepsilon} \right) e^{\frac{K\|v\|^4}{2\varepsilon}} \leq 1 + \left(\frac{K\|v\|^4}{2\varepsilon} \right) e^{\frac{\|v\|^2}{4\varepsilon}},$$

where the second inequality follows from the assumption $\varepsilon_0^2 < \frac{1}{2K}$ (see Remark 3.2). Therefore, we have

$$e^{-\frac{\|v\|^2}{2\varepsilon}} \leq k_\varepsilon(x, \exp_x(v)) \leq e^{-\frac{\|v\|^2}{2\varepsilon}} + \left(\frac{K\|v\|^4}{2\varepsilon}\right) e^{-\frac{\|v\|^2}{4\varepsilon}}$$

and in particular,

$$\begin{aligned} \left| \int_{\|v\| < r(x)} \left(k_\varepsilon(x, \exp_x(v)) - e^{-\frac{\|v\|^2}{2\varepsilon}} \right) (f(x) - f(\exp_x(v))) \sqrt{|\det[g(v)]|} dv \right| &\leq \frac{K}{2\varepsilon} \int_{\|v\| < r(x)} e^{-\frac{\|v\|^2}{4\varepsilon}} O(\|v\|^5) dv \\ &\lesssim \frac{K}{\varepsilon} \int_{\mathbb{R}^m} e^{-\frac{\|v\|^2}{4\varepsilon}} \|v\|^5 dv \\ &\lesssim K\varepsilon^{\frac{m+3}{2}}. \end{aligned}$$

Plugging in the Taylor expansions (34) and (35),

$$\begin{aligned} &\int_{\|v\| < r(x)} e^{-\frac{\|v\|^2}{2\varepsilon}} (f(x) - f(\exp_x(v))) \sqrt{|\det[g(v)]|} dv \\ &= - \int_{\|v\| < r(x)} e^{-\frac{\|v\|^2}{2\varepsilon}} \left(\langle \text{grad} f(x), v \rangle + \frac{1}{2} \text{Hess}_x f(v, v) + O(\|v\|^3) \right) \left(1 - \frac{\text{Ric}_x(v, v)}{6} + O(\|v\|^3) \right) dv \\ &= -\frac{1}{2} \int_{\|v\| < r(x)} e^{-\frac{\|v\|^2}{2\varepsilon}} \text{Hess}_x f(v, v) dv + O\left(\varepsilon^{\frac{m+3}{2}}\right) \\ &= (2\pi\varepsilon)^{m/2} I_2(x) + O\left(\varepsilon^{\frac{m+3}{2}}\right), \end{aligned}$$

where

$$\int_{\|v\| < r(x)} e^{-\frac{\|v\|^2}{2\varepsilon}} \langle \text{grad} f(x), v \rangle \left(1 - \frac{\text{Ric}_x(v, v)}{6} \right) dv = 0$$

by symmetry. It follows that there exists $C > 0$ such that

$$|I_1(x) - I_2(x)| \leq C \max(1, K) \varepsilon^{3/2} =: R_2(\varepsilon).$$

3. Approximation of an integral on a ball with an integral over \mathbb{R}^m . By Lemma C.1,

$$I_2(x) = \frac{1}{2(2\pi\varepsilon)^{m/2}} \left(\frac{\text{area}(\mathbb{S}^{m-1}) \Delta_g f(x)}{m} \right) \int_0^r e^{-\frac{y^2}{2\varepsilon}} y^{m+1} dy.$$

Now observe that

$$\begin{aligned} \frac{\text{area}(\mathbb{S}^{m-1})}{m} \int_0^r e^{-\frac{y^2}{2\varepsilon}} y^{m+1} dy &= \frac{\text{area}(\mathbb{S}^{m-1})}{m} \left(\int_0^\infty e^{-\frac{y^2}{2\varepsilon}} y^{m+1} dy - \int_{r(x)}^\infty e^{-\frac{y^2}{2\varepsilon}} y^{m+1} dy \right) \\ &= \frac{1}{m} \int_{\mathbb{R}^m} e^{-\frac{\|v\|^2}{2\varepsilon}} \|v\|^2 dv - \frac{\text{area}(\mathbb{S}^{m-1})}{m} \int_{r(x)}^\infty e^{-\frac{y^2}{2\varepsilon}} y^{m+1} dy \\ &= (2\pi\varepsilon)^{m/2} \varepsilon - \frac{\text{area}(\mathbb{S}^{m-1})}{m} \int_{r(x)}^\infty e^{-\frac{y^2}{2\varepsilon}} y^{m+1} dy, \end{aligned}$$

where the last line is obtained by computing the variance of a multi-dimensional Gaussian. It follows that

$$\left| I_2(x) - \frac{\varepsilon}{2} \Delta_g f(x) \right| \leq R_3(\varepsilon),$$

and (26) follows from the triangle inequality. \square

APPENDIX B. PROOF OF LEMMA 5.1

Proof of Lemma 5.1. It suffices to prove the statement for $\theta \in (0, \pi]$ and when $\text{supp } \iota_{r_1}(\theta) \cap \text{supp } \iota_{r_1}(0)$ is non-empty. The latter condition is equivalent to the condition

$$\left| \frac{\sin\left(\frac{\theta}{2}\right)}{r_1} \right| < 1.$$

Similar computations to Section 4.3 give us

$$\|\iota_r(\theta) - \iota_r(0)\|_{L^1} = \frac{1}{2r} \left(\pi r^2 - 2 \left(r^2 \arccos\left(\frac{\sin\left(\frac{\theta}{2}\right)}{r}\right) - \sin\left(\frac{\theta}{2}\right) \sqrt{r^2 - \sin^2\left(\frac{\theta}{2}\right)} \right) \right) \quad (36)$$

$$= \frac{\pi r}{2} - r \arccos\left(\frac{\sin\left(\frac{\theta}{2}\right)}{r}\right) + \sin\left(\frac{\theta}{2}\right) \sqrt{1 - \left(\frac{\sin\left(\frac{\theta}{2}\right)}{r}\right)^2}. \quad (37)$$

Taking $f(r, \theta) := \|\iota_r(\theta) - \iota_r(0)\|_{L^1}$, it now suffices to show that

$$\frac{\partial f}{\partial r}(r, \theta) > 0$$

for all r, θ such that $\theta \in (0, \pi]$ and $r > \sin\left(\frac{\theta}{2}\right)$. Indeed, taking the derivative of (37) gives us

$$\frac{\partial f}{\partial r}(r, \theta) = \frac{\pi}{2} - \arccos\left(\frac{\sin\left(\frac{\theta}{2}\right)}{r}\right) + \frac{1}{\sqrt{1 - \left(\frac{\sin\left(\frac{\theta}{2}\right)}{r}\right)^2}} \left(\left(\frac{\sin\left(\frac{\theta}{2}\right)}{r}\right)^3 - \left(\frac{\sin\left(\frac{\theta}{2}\right)}{r}\right) \right).$$

Making the change of variables $x = \frac{\sin\left(\frac{\theta}{2}\right)}{r}$, it remains to show that

$$g(x) := \frac{\pi}{2} - \arccos(x) + \frac{x^3 - x}{\sqrt{1 - x^2}} = \frac{\pi}{2} - \arccos(x) - x\sqrt{1 - x^2} > 0$$

for all $x \in (0, 1)$. This follows from observing that $g(0) = 0$ and

$$g'(x) = \frac{1}{\sqrt{1 - x^2}} + \frac{x^2}{\sqrt{1 - x^2}} - \sqrt{1 - x^2} = \frac{2x^2}{\sqrt{1 - x^2}} > 0$$

for all $x \in (0, 1)$. □

APPENDIX C. AUXILIARY LEMMAS

The following lemma is helpful for computations; we include a proof of it for completeness.

Lemma C.1. *Let $m \in \mathbb{N}$ and $r > 0$. For any $m \times m$ symmetric matrix A and integrable function $h: (0, r) \rightarrow \mathbb{R}$,*

$$\int_{B_r(0)} h(\|v\|) v^T A v dv = \frac{\text{area}(\mathbb{S}^{m-1}) \text{Tr}(A)}{m} \int_0^r h(x) x^{m+1} dx.$$

Proof. By considering the spectral decomposition $A = U\Lambda U^T$, we obtain

$$\begin{aligned} \int_{B_r(0)} h(\|v\|)v^T A v dv &= \text{area}(\mathbb{S}^{m-1}) \int_0^r h(x)x^2 \left(\int_{\mathbb{S}^{m-1}} \varphi^T A \varphi d\mu_{\mathbb{S}^{m-1}}(\varphi) \right) x^{m-1} dx \\ &= \text{area}(\mathbb{S}^{m-1}) \left(\int_{\mathbb{S}^{m-1}} \varphi^T \Lambda \varphi d\mu_{\mathbb{S}^{m-1}}(\varphi) \right) \left(\int_0^r h(x)x^{m+1} dx \right) \\ &= \frac{\text{area}(\mathbb{S}^{m-1}) \text{Tr}(A)}{m} \int_0^r h(x)x^{m+1} dx. \end{aligned}$$

□

Lemma C.2. *Suppose (\mathcal{M}, g) is a Riemannian manifold, (X, d) is a metric space and $\iota: \mathcal{M} \rightarrow X$ is an embedding. Then for any $x \in \mathcal{M}$ and $R > 0$,*

$$\beta(x, R) := \inf_{\substack{y \in \mathcal{M} \\ d_g(y, x) \geq R}} d(\iota(y), \iota(x))$$

is strictly positive.

Proof. Since $B_R(x) := \{y \in \mathcal{M}: d_g(y, x) < R\}$ is open and ι is an embedding, $\iota(B_R(x))$ is open in $\iota(\mathcal{M})$ with respect to the subspace topology from (X, d) . Suppose for contradiction that $\beta(x, R) = 0$. Then for all $s > 0$,

$$\tilde{B}_s(\iota(x)) := \{z \in \iota(\mathcal{M}): d(z, \iota(x)) < s\}$$

contains $\iota(y)$ for some $y \notin B_R(x)$. Thus $\iota(x) \in \iota(B_R(x))$, but there does not exist $s > 0$ such that $\tilde{B}_s(\iota(x)) \subset \iota(B_R(x))$. This implies that $\iota(B_R(x))$ is not open in $\iota(\mathcal{M})$ with the subspace topology, which is a contradiction. □

Lemma C.3. *Let \mathcal{M} be a smooth, compact manifold and suppose d is a metric on \mathcal{M} such that d^2 is C^{k+3} on a neighborhood of $D_{\mathcal{M}}$ for some $k \geq 4$. Then there exist $\kappa, \rho > 0$ satisfying the required conditions for Theorem 3.3.*

Proof. Let $\mathcal{E} \subset T\mathcal{M}$ be an open neighborhood of $\mathcal{M} \times \{0\}$ on which the exponential map \exp is defined. Since \exp is C^k , by the inverse function theorem,

$$\begin{aligned} F: \mathcal{E} &\rightarrow \mathcal{M} \times \mathcal{M} \\ (p, v) &\mapsto (p, \exp_p(v)) \end{aligned}$$

has a local C^k inverse around (p, p) for each $p \in \mathcal{M}$. Fix any $p \in \mathcal{M}$. Recall that a subset $V \subset \mathcal{M}$ is *strongly convex* if for any $x, y \in \bar{V}$, there exists a unique length-minimizing geodesic γ from x to y , and the interior of $\text{Im } \gamma$ is contained in V [23, p. 74]. We claim that for small enough $r > 0$, $B_r(p)$ is strongly convex; although [23] works with smooth Riemannian manifolds, the argument in [23, Chapter 3, Section 4] holds here as well. Therefore we can take $r > 0$ so that there exists a C^k inverse F^{-1} for F on an open neighborhood of $\overline{B_r(p)} \times \overline{B_r(p)}$, $d^2 \in C^{k+3}(\overline{B_r(p)} \times \overline{B_r(p)})$ and $B_r(p)$ is strongly convex.

Since \mathcal{M} is compact, we can cover \mathcal{M} with finitely many balls of the form $B_{r/2}(p)$, where r satisfies the conditions in the previous sentence. For any $x \in B_{r/2}(p)$ and $y \in \mathcal{M}$ such that $d_g(x, y) < \frac{r}{2}$, there exists a length-minimizing geodesic γ from x to y by the strong convexity of $B_r(p)$, and d^2 is C^4 on $\text{Im } \gamma \times \text{Im } \gamma$ since $\text{Im } \gamma \subset B_r(p)$. Thus, it suffices to prove that there exists $\tilde{\kappa} > 0$ such that

$$\left| h_{(x,v)}^{(4)}(t) \right| < \tilde{\kappa}$$

for all $x \in B_{r/2}(p)$, unit-norm $v \in T_x\mathcal{M}$ and $|t| < \frac{r}{2}$.

This follows almost immediately from considering $h_{(x,v)}(t) = d^2(x, \exp_x(tv))$ as a map h on the compact set $S := \{(x, v) \in T\mathcal{M} : x \in \overline{B_{r/2}(p)}, g_x(v, v) = 1\} \times [-\frac{r}{2}, \frac{r}{2}]$:

$$\begin{aligned} h : S &\rightarrow \mathbb{R} \\ ((x, v), t) &\mapsto h_{(x,v)}(t). \end{aligned}$$

Since h is C^k for $k \geq 4$ on S ,

$$\sup_{((x,v),t) \in S} \left| h_{(x,v)}^{(4)}(t) \right| < \infty.$$

□